AD-A034 909 AEROCHEM RESEARCH LABS INC PRINCETON N J F/G 7/4
KINETICS AND KINETIC SPECTROSCOPY OF THE SN/N(SUB 2)O ELECTRONI--ETC(U)
NOV 76 W FELDER, A FONTIJN F29601-75-C-0118
UNCLASSIFIED AFWL-TR-76-162 NL

1 OF 1
AD-A
034 909

END
DATE
FILMED
3-7-77
NTIS

KINETICS AND KINETIC SPECTROSCOPY OF THE Sn/N(sub 2)O ELECTRONIC TRANSITION CHEMICAL LASER CANDIDATE REACTION

AeroChem Research Laboratories, Inc.
Princeton, New Jersey

November 1976

AFWL-TR-76-162

AFWL-TR-
76-162

KINETICS AND KINETIC SPECTROSCOPY OF THE Sn/N_2O ELECTRONIC TRANSITION CHEMICAL LASER CANDIDATE REACTION

AreoChem Research Laboratories, Inc.
P.O. Box 12
Princeton, NJ 08540

November 1976

Final Report

Approved for public release; distribution unlimited.

Prepared for

DEFENSE ADVANCED RESEARCH PROJECT AGENCY
Arlington, VA 22209

AIR FORCE WEAPONS LABORATORY
Air Force Systems Command
Kirtland Air Force Base, NM 87117

This final report was prepared by AreoChem Research Laboratories, Inc., Princeton, NJ, under Contract F29601-75-C-0118, Job Order 12560306, with the Air Force Weapons Laboratory, Kirtland AFB, NM. Capt Chester J. Dymek, Jr. (ALC) was the Project Officer-in-Charge.

This technical report has been reviewed and is approved for publication.

This report has been reviewed by the Information Office (OI) and is releasable to the National Technical Information Service (NTIS). At NTIS, it will be available to the general public, including foreign nations.

Chester J Dymek Jr

CHESTER J. DYMEK, JR.
Capt, USAF
Project Officer

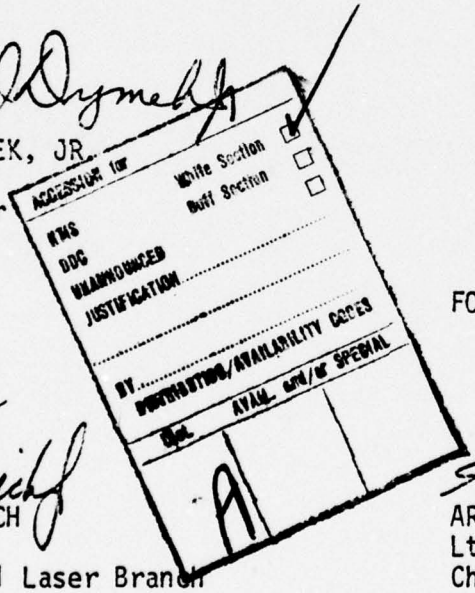

FOR THE COMMANDER

Carl A Forbrich

CARL A. FORBRICH
Maj, USAF
Chief, Chemical Laser Branch

Armand D Maio

ARMAND D. MAIO
LtColonel, USAF
Chief, Advanced Laser Technology Division

DO NOT RETURN THIS COPY. RETAIN OR DESTROY.

UNCLASSIFIED

SECURITY CLASSIFICATION OF THIS PAGE *(When Data Entered)*

REPORT DOCUMENTATION PAGE		READ INSTRUCTIONS BEFORE COMPLETING FORM
1. REPORT NUMBER AFWL-TR-76-162	2. GOVT ACCESSION NO.	3. RECIPIENT'S CATALOG NUMBER
4. TITLE *(and Subtitle)* KINETICS AND KINETIC SPECTROSCOPY OF THE Sn/N_2O ELECTRONIC TRANSITION CHEMICAL LASER CANDIDATE REACTION		5. TYPE OF REPORT & PERIOD COVERED Final Report 6. PERFORMING ORG. REPORT NUMBER
7. AUTHOR(s) William Felder, Arthur Fontijn		8. CONTRACT OR GRANT NUMBER(s) F29601-75-C-0118
9. PERFORMING ORGANIZATION NAME AND ADDRESS AreoChem Research Laboratories, Inc. P.O. Box 12 Princeton, NJ 08540		10. PROGRAM ELEMENT, PROJECT, TASK AREA & WORK UNIT NUMBERS 62301E 12560306
11. CONTROLLING OFFICE NAME AND ADDRESS Defense Advanced Research Project Agency 1400 Wilson Boulevard Arlington, VA 22209		12. REPORT DATE November 1976 13. NUMBER OF PAGES 48
14. MONITORING AGENCY NAME & ADDRESS*(if different from Controlling Office)* Air Force Weapons Laboratory (ALC) Kirtland AFB, NM 87117		15. SECURITY CLASS. *(of this report)* Unclassified 15a. DECLASSIFICATION/DOWNGRADING SCHEDULE

16. DISTRIBUTION STATEMENT *(of this Report)*

Approved for public release; distribution unlimited.

17. DISTRIBUTION STATEMENT *(of the abstract entered in Block 20, if different from Report)*

18. SUPPLEMENTARY NOTES

19. KEY WORDS *(Continue on reverse side if necessary and identify by block number)*

Chemical Lasers
Chemical Kinetics
Chemiluminescence
Electronic Quenching
SnO
Metal Atoms

20. ABSTRACT *(Continue on reverse side if necessary and identify by block number)*

Studies were performed in the AeroChem High-Temperature Fast-Flow Reactors. A titration technique was developed for the measurement of absolute [Sn]. For the the overall reaction $Sn + N_2O \xrightarrow{(1)} SnO(all\ states) + N_2$, $k_1(300\text{-}1000K) = (1 \pm 4) \times 10^{-11} \exp[-(3000 \pm 1000)/T]$ ml molecule^{-1} sec^{-1}. Only two SnO excited states, $a^3\Sigma$ and $A^3\Pi$, are populated in this reaction. The photon yield

(continued on reverse)

DD FORM 1 JAN 73 1473 EDITION OF 1 NOV 65 IS OBSOLETE

UNCLASSIFIED

SECURITY CLASSIFICATION OF THIS PAGE *(When Data Entered)*

(Block 20 continued)

$\Phi(a) = 0.51 \pm 0.22$ from 500-930; the rate coefficient for photon emission, $k_{h\nu}$, has the same dependence on T as k_1 since $k_{h\nu}(T) = k_1(T)\Phi(T)$. $\Phi(A)$ increases from 0.04 at 500 K to 0.16 at 930 K. At 1350 K only $SnO(B^3\Pi)$ and $(D^1\Pi)$ are populated, apparently due to complete heterogeneous N_2O dissociation followed by $Sn + O + M \rightarrow SnO(B,D) + M$. These observations imply that $SnO(B^3\Pi, A^3\Pi)$ may not be different angular momentum components of the same triplet state as their spectroscopic labels indicate. Rate coefficients, k_Q, for quenching were measured for $SnO(a^3\Sigma^+)$: $k_Q^{N_2} \leq 0.6 \times 10^{-16}$, $k_Q^{Ar} \leq 1.0 \times 10^{-16}$, $k_Q^{N_2O} \leq 1.0 \times 10^{-14}$, and $k_Q^{Sn} \leq 1.2 \times 10^{-12}$ ml molecule^{-1} sec^{-1}, assuming $\tau_{rad} = 10^{-3}$ sec. For $SnO(A^3\Pi)$: $\tau_A k_Q^{N_2} = 1.3 \times 10^{-18}$, $\tau_A k_Q^{Ar} \leq 3.2 \times 10^{-19}$, $\tau_A k_Q^{N_2O} \leq 1.4 \times 10^{-17}$, and $\tau_A k_Q^{Sn} \leq 1.3 \times 10^{-15}$ ml molecule^{-1}. Indications of SnO(a,A) quenching by a reaction product are obtained; however, this product is apparently not SnO but results from further reaction, suggesting it should not interfere with laser operation. Preliminary gain calculations assuming no quenching and a Boltzmann ground state distribution suggest gain of $\gtrsim$ 0.1% cm^{-1} for SnO(a, ~~O-X~~, $v'' \geq 2$) in the R branch ($J' = 35$) (at 530-600 nm), more than adequate for a practical device.

PREFACE

The authors wish to acknowledge the work of J.J. Houghton and R. Ellison on the experiments reported herein. We thank Dr. R.K. Gould for making initial gain calculations and for useful comments on all phases of the work.

CONTENTS

ILLUSTRATIONS

TABLES

SECTION I

INTRODUCTION

The purpose of this work is to provide more detailed information on the reaction

$$Sn + N_2O \rightarrow SnO(\text{all states}) + N_2 \qquad (1)$$

to evaluate its potential as an electronic transition chemical laser pumping reaction.

Under a previous contract with the Naval Research Laboratory we showed that this reaction is promising for this application (ref. 1) on the basis of the large (> 10%) fraction of reactions leading to a single electronically excited state, $SnO(a^3\Sigma^+)$. The radiative lifetime, τ_a, of this state is known (refs. 2,3) to be 2.5×10^{-4} sec in a solid matrix and may on this basis be estimated to be $10^{-3\pm0.5}$ sec in the gas phase. Since radiative lifetimes on the order of 10^{-3} to 10^{-5} sec are considered ideal for electronic lasing action the Sn/N_2O reaction appeared, a priori, to be a good candidate. In the present work measurements on the temperature dependence of the Sn/N_2O overall rate coefficient, k_1, and rate coefficients for quenching of $SnO(a^3\Sigma^+)$ and $(A^3\Pi)$ were performed as were mechanistic studies and a determination of absolute photon yields. The studies were carried out using AeroChem High-Temperature Fast-Flow Reactors (HTFFR) (refs. 1,4 thru 8). The results are evaluated in terms of laser development.

It should be stated at the outset that currently there is considerable confusion as to the correct identity of the second and third (in order of excitation energy) excited states of SnO. In order not to add to the melee of identifications, we have for this report used the most recent proposal, which is that by Zare's group (ref. 9). Thus the four lowest excited states are identified as $a^3\Sigma^+$ (1), $A^3\Pi$ (0^+), $B^3\Pi$ (1) and $D^1\Pi$. However, in section IV.C.3 we discuss evidence obtained in the present work which suggests that this identification is also incorrect.

SECTION II

EXPERIMENTAL

A. Apparatus

Figures 1 to 3 show the modifications of the HTFFR used in this work. Figure 1 is a diagram of an HTFFR, consisting of a 1 m long alumina flow tube heated in three separate sections by directly wound Pt/40% Rh resistance wire, which was used for measurements in the $\approx$ 700 to $\approx$ 1300 K range (this reactor can achieve temperatures (refs. 4, 6, 10) up to $\approx$ 1900 K). Figure 2 shows the HTFFR used for $\approx$ 300 K measurements; it consists of two sections, an upstream $\approx$ 30 cm long heated alumina flow tube source section which is maintained at $\approx$ 1700 K to vaporize Sn and a cooled reaction zone section (ref. 10). In the HTFFR of figure 3 this cooled section is replaced by a $\approx$ 30 cm long heated alumina flow tube; this version of the HTFFR was used for measurements in the 500 to 1000 K range.

Sn is vaporized from a separately heated source placed in the upstream end of the reactor. This source was usually a resistance-heated alumina crucible (1.5 cm diam x 2 cm deep) filled with Sn metal and provided [Sn] on the order of 10^{11} ml^{-1}. For experiments on Sn quenching and titrations, where

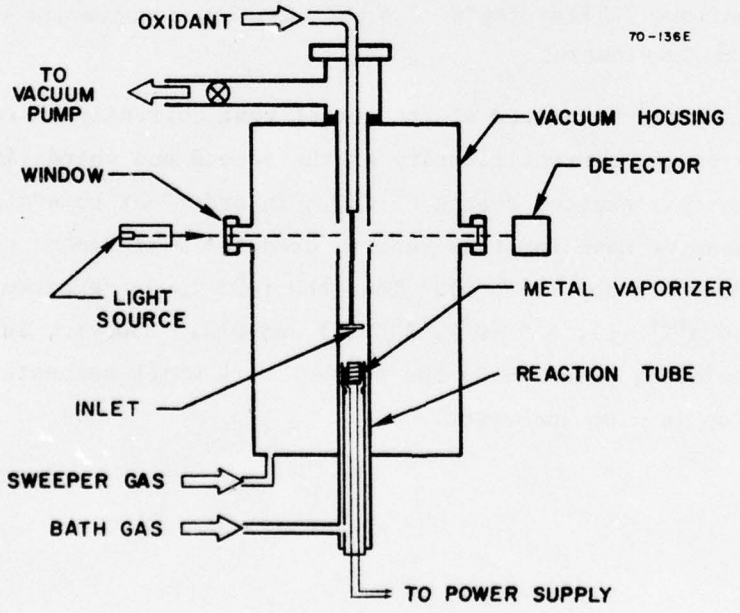

Figure 1. Diagram of an HTFFR

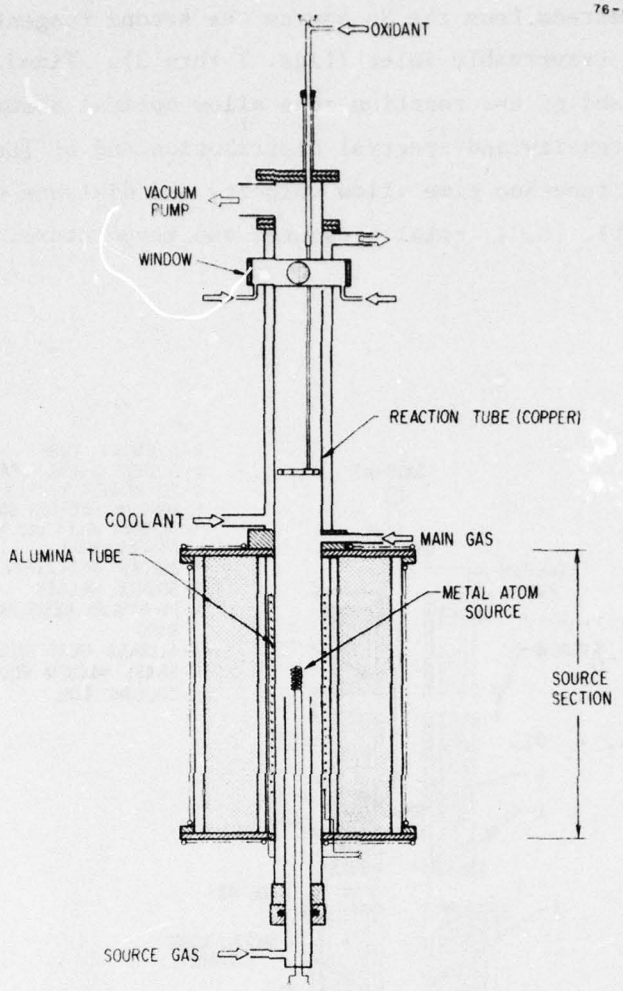

Figure 2. Modular HTFFR for kinetic/spectroscopic measurements in the 300 to 500 K range

[Sn] > 1 x 10^{13} ml^{-1} was required, a modified source was developed. This source consists of a three-stranded, coiled W-filament wick, partially immersed in the alumina crucible. The W-filament wick is resistance heated, using the liquid Sn as an electrical contact. Sn wets the W-filament and the higher flux required can be obtained from this larger surface area. The bath gas used for the 'low' [Sn] experiments was N_2, for 'high' [Sn] it was found necessary to use Ar instead. This is probably due mainly to the higher heat capacity of N_2 which causes it to cool the Sn vaporizer more efficiently than Ar resulting in a smaller Sn flux.

Downstream from the Sn source the second reagent (e.g., N_2O) is added through a traversable inlet (figs. 1 thru 3). Fixed viewing ports at the downstream end of the reaction zone allow optical observations of chemiluminescence intensity and spectral distribution and of [Sn] concentration as functions of reaction time (flow velocity and distance of inlet form observation port), [N_2O], total pressure, and temperature.

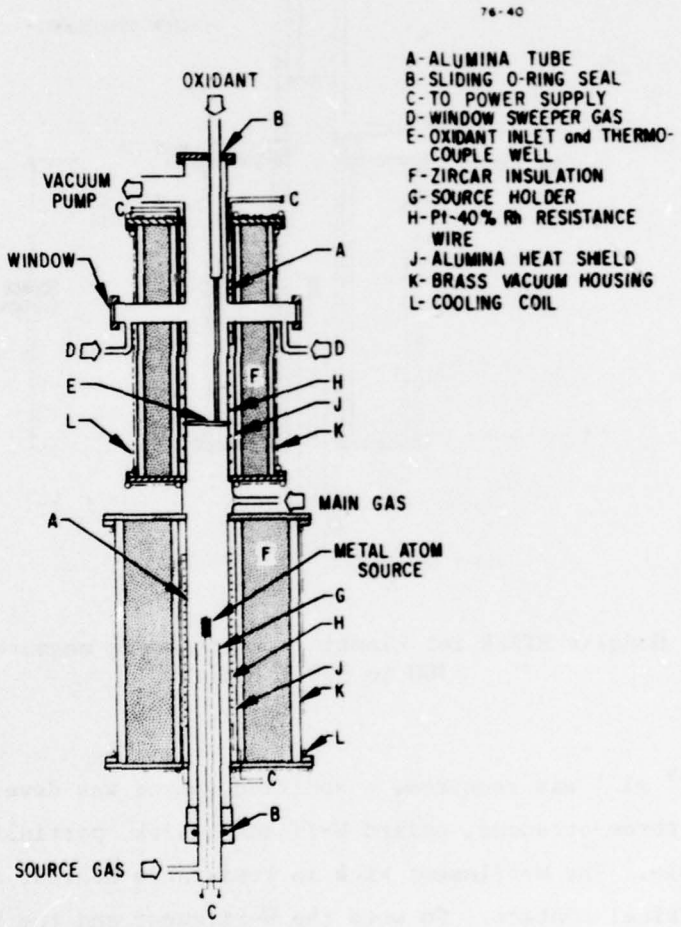

Figure 3. Modular HTFFR for kinetic/spectroscopic measurements in the 500 to 1350 K range

Figure 4 shows a cross-section of the observation plane; the layout is described in detail in reference 1. [Sn] is monitored via absorption of its resonance line radiation emitted by a Sn hollow cathode lamp. The output

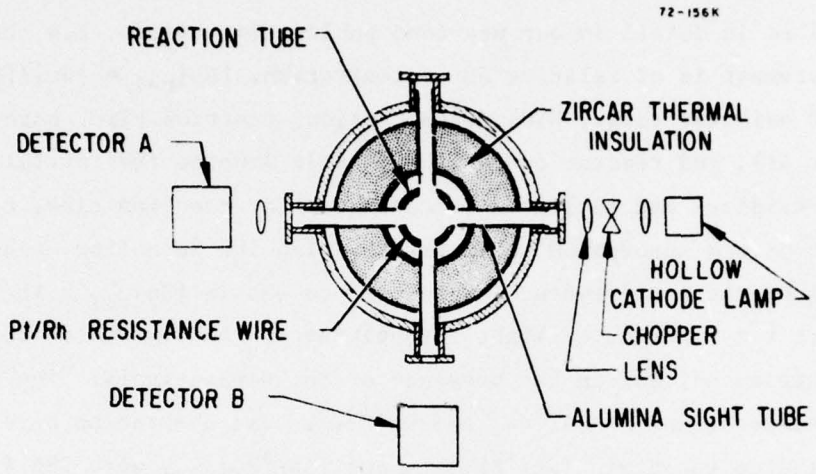

Figure 4. Cross-section of the observation plane of an HTFFR. Reaction tube, 2.5 cm i.d.; reaction tube observation ports 1 cm diam. Detector A for Sn absorption and SnO chemiluminescence spectral intensity measurements. Detector B for monitoring and normalizing chemiluminescence intensity measurements. Remaining port used for visual observation of chemiluminescence and blocked otherwise.

of this lamp is chopped at 140 Hz and, after passing through the flow tube, measured by Detector A, a Minuteman 1/2 Czerny-Turner monochromator with thermoelectrically cooled EMI-9558QA or RCA C31034 photomultiplier tubes (PMT), the signals from which are processed with a lock-in amplifier. Detector A is also used for chemiluminescence spectral measurements, in which case the emission from the hollow cathode lamp is blocked and the PMT output is amplified by a Keithly 417 picoammeter. The picoammeter output is fed to an integrating strip chart recorder. Detector B is a HTV R212 PMT which monitors the chemiluminescence over its entire wavelength response region. This monitor signal is used to normalize the output from Detector A to allow compensation for up to $\approx$ 30% system intensity excursions due to metal atom density fluctuations when taking

chemiluminescence spectra. The observed magnitude of such excursions is typically less than 5%.

B. Methods and Procedures

1. Rate Coefficient Measurements

The procedures used in determining rate coefficients in the HTFFR have been described in detail in our previous publications (refs. 1,4 thru 8,10). The basic measurement is of relative Sn concentration, $[Sn]_{rel} = [Sn]/[Sn]_o$, as a function of oxidizer (e.g., N_2O) concentration, reaction time, bath gas pressure (N_2 or Ar), and reactor temperature; $[Sn]_o$ denotes the initial [Sn] in the absence of oxidizer and [Sn], the concentration at reaction time, t. $[Sn]_{rel}$ is determined from absorption measurements using the Sn-hollow cathode lamp. In absorption, the Lambert-Beer law is used to obtain $[Sn]_{rel} \propto \ln(I_o/I)$, where I_o and I are the transmitted light intensities in the absence of Sn (excess oxidizer introduced) and in the presence of Sn, respectively. The present work investigated reactions of $Sn(^3P_o)$ and $Sn(^3P_1)$. The absorption wavelengths used in these studies to obtain $[Sn(^3P_o)]_{rel}$ and $[Sn(^3P_1)]_{rel}$ were 286.4 nm ($5p^2\ ^3P_o \rightleftarrows 6s\ ^3P_1^o$) and 300.9 nm ($5p^2\ ^3P_1 \rightleftarrows 6s\ ^3P_1^o$), respectively (ref. 11). To measure overall rate coefficients, only knowledge of the relative concentration of Sn is needed because the experiments are performed under conditions in which [oxidizer] >> [Sn], i.e., under pseudo first-order kinetic conditions. However, measurement of photon yields, Φ, and rate coefficients for light emission, $k_{h\nu}$, require absolute [Sn] (section II.B.2).

Rate coefficients were obtained from measurements of $[Sn(^3P_J)]_{rel}$ in the traversing inlet mode (refs. 1,4 thru 8,10). In this mode, pseudo first-order rate coefficients, $k_{ps_1} = -d \ln[Sn(^3P_J)]_{rel}/dt$ are measured. The bimolecular rate coefficients are then obtained from plots of k_{ps_1} vs. [oxidizer]. Reaction time $t = x/\eta\bar{v}$, where x is the distance from the oxidizer inlet to the observation plane windows (see figs. 1 thru 3), $\bar{v}$, the average gas velocity, and η is a factor equal to 1 for plug flow and approximately equal to 1.6 for parabolic flow. For our calculations in this work we have again (refs. 1,5 thru 8) taken η to be 1.3 ± 0.3.

2. Photon Yield Measurements

We have previously described the methods for obtaining Sn/N_2O photon

yields, Φ (ref. 1). The photon yield is defined as the number of photons emitted per Sn/N_2O reaction event; its value is determined by measuring the absolute total intensity of the Sn/N_2O chemiluminescence and dividing this by the flux of the limiting reagent into the reaction zone. The limiting reagent is either Sn, when $[N_2O] >> [Sn]$, or N_2O, when $[Sn] \geq 10[N_2O]$. These two cases are referred to as oxidizer-in-excess and metal-in-excess (refs. 12, 13) measurements of Φ, respectively. The actual measurement of Φ consists of three steps:

(i) Determination of the spectral distribution of the chemiluminescence (Detector A, fig. 4). The spectra obtained are integrated over the full wavelength range (using the integrating recorder) and corrected for wavelength response and absolute sensitivity of the detector by comparison with the O/NO glow (ref. 14). For $300 \leq \lambda \leq 400$ nm, detector response is calibrated by extrapolating the O/NO data using the manufacturer's specifications for wavelength response of the monochromator grating and PMT. These procedures yield the absolute intensity I_S(a, A, B, or D) of that fraction of the total chemiluminescent glow which lies within the viewing aperture of the detector. In these experiments, this aperture was 2 cm at its widest dimension along the direction of flow in the HTFFR (figs. 1 thru 3).

(ii) Determination of the spatial distributions of the chemiluminescence. The fraction of the total chemiluminescent glow measured in (i) is determined by measuring the total volume of the chemiluminescent glow. This is done by measuring the intensity of representative peaks in each of the SnO band systems ($a^3\Sigma-$, $A^3\Pi-$, $B^3\Pi-$, $D^1\Pi-X^1\Sigma$), as a function of distance of the N_2O inlet from the observation window. Plots such as shown in figure 5, illustrating the a–X (0,4) transition at 579 nm (ref. 15) are derived from these measurements for each band system. The areas under such curves A_{TOT} (a, A, B, or D) are proportional to the total (volume integrated) chemiluminescence intensity in each band system; the area under the cross-hatched portion of the curve is proportional to the fraction of total intensity measured in the spectra of (i), A_S(a, A, B, D). Hence, the absolute total intensity of the chemiluminescence is given by

$$I_{TOT} = I_S \times \frac{A_{TOT}}{A_S} \qquad (2)$$

for each band system.

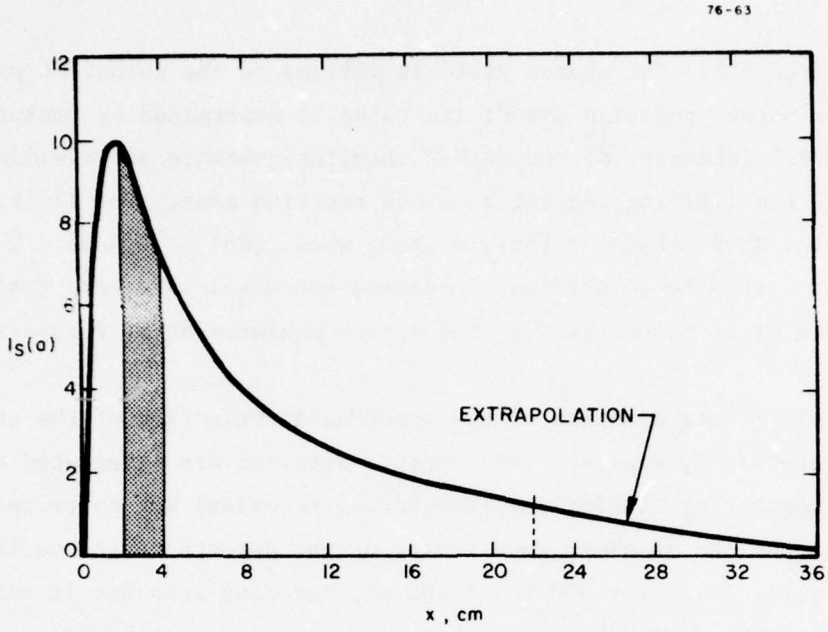

Figure 5. Plot of intensity of $a^3\Sigma - X^1\Sigma$ (0,4) band at 579 nm vs. distance from observation plane in HTFFR. Cross-hatched area is fraction of total glow observed in spectral measurement.
T = 920 K, $[N_2] = 1.6 \times 10^{17}$ ml^{-1} (15 torr), $[N_2O] = 1.9 \times 10^{15}$ ml^{-1}, $[Sn]_o = 2.0 \times 10^{11}$ ml^{-1}, $\bar{v}$ = 25 m/sec.

Depending upon reactant concentrations, linear flow velocities, and reaction zone temperatures, the length of the chemiluminescent glow (to decay to $\approx$ 1% of the peak intensity) varied from $\approx$ 8 cm to beyond the traverse range of the N_2O inlet (22 cm). In the latter case, extrapolations of the intensity vs. distance curves were used to determine the glow integrated intensity (fig. 5). For most of the data reported here, these extrapolations amounted to < 20% of the total area under the intensity vs. distance curves and could readily be made by hand. The most extreme conditions encountered in this work were those used in the metal-in-excess Φ measurements and in the Sn quenching experiments; treatment of the intensity vs. distance curves for these experiments will be discussed below (sections III.C. and III.D.2).

(iii) Determination of flux of limiting reagent. The definition of flux is $[R]\eta\bar{v}a$, where [R] is the concentration of the limiting reagent, $\bar{v}$ is the average gas velocity, a is the HTFFR reaction tube cross-sectional area, and η is defined above (section II.B.1). In the metal-in-excess Φ measurements, where

N_2O is the limiting reagent, the measurement of $[N_2O]$ follows directly from its volume flow rate into the reaction zone. The measurement of $[Sn]_{abs(olute)}$ is more complicated, and we have used two methods for its determination: resonance absorption which is suitable for $2 \times 10^{10} \leq [Sn] \leq 8 \times 10^{11}$ ml^{-1} and a chemical titration with NO_2 which is suitable for $[Sn] \geq 1 \times 10^{13}$ ml^{-1}. In the absorption method $[Sn]_{abs}$ is calculated from the observed attenuation of the 286.4 nm resonance line and the best literature value f number (ref. 16) (f = 0.186). The calculation method followed assumes Doppler broadened emission and absorption lines with the absorption line Doppler temperature being the HTFFR reaction zone temperature and the emission line Doppler temperature assumed to be $\tilde{\sim}$ 600 K, in accord with the findings of deGalan (ref. 17). The calculation procedure is given in reference 18, Appendix IV. It is identical with the method used by Kaufman and coworkers (ref. 19) in their determination of the f-numbers of the N atom and O atom resonance lines. We previously estimated the accuracy of this method to be about a factor of 2 (ref. 1). By comparing Φ measurements in the metal-in-excess mode with Φ measurements in the oxidizer-in-excess mode, we have obtained evidence in this work that the accuracy is probably 42%. (section III.C.) for Sn.

The second method used to determine $[Sn]_{abs}$ was chemical titration with NO_2 using the Sn/N_2O reaction as a chemiluminescence indicator. A separate discussion of this method is given below (section II.B.3). It was found suitable for $[Sn] \geq 1 \times 10^{13}$ ml^{-1} and was used in determining values of $[Sn]_{abs}$ required in Sn-quenching experiments (section III.D.2).

With the determination of [R], the photon yield for any band system is calculated from

$$\Phi = I_{TOT}/[R]\eta\bar{\nu}a \qquad (3)$$

The denominator is the amount of limiting reagent, R, reacted sec^{-1} (equal to the amount entering the reaction zone) and the numerator is the number of photons sec^{-1} emitted.

3. Titration of Sn to Determine $[Sn]_{abs}$

To determine $[Sn]_{abs}$ a chemiluminescence titration procedure was developed by analogy to the well established titration procedures for atoms of

non-refractory species, e.g., N, O, H, Cl, in common use in flow tube work (ref. 20). Titrations were carried out using the rapid (section III.B.) reaction

$$Sn + NO_2 \rightarrow Products$$

with the Sn/N_2O chemiluminescence as indicator. NO_2 was introduced through the movable inlet distributor ring at the upstream end of the HTFFR reaction zone. Approximately 1 cm upstream of the observation port a flow of N_2O such that $[N_2O] \doteq 1 \times 10^{15}$ ml^{-1} >> [Sn] was also introduced through a hook-shaped second inlet. The chemiluminescence was observed with Detector A, and its intensity, with $[N_2O]$ in excess, is proportional to the [Sn] arriving at the N_2O inlet. As NO_2 is incrementally added to the flow, the [Sn] at the observation port is reduced, and the chemiluminescence extinguished.

Figure 6 shows a typical plot of a—X indicator chemiluminescence intensity, I, against $[NO_2]$ normalized to the value I_o when $[NO_2] = 0$. If the

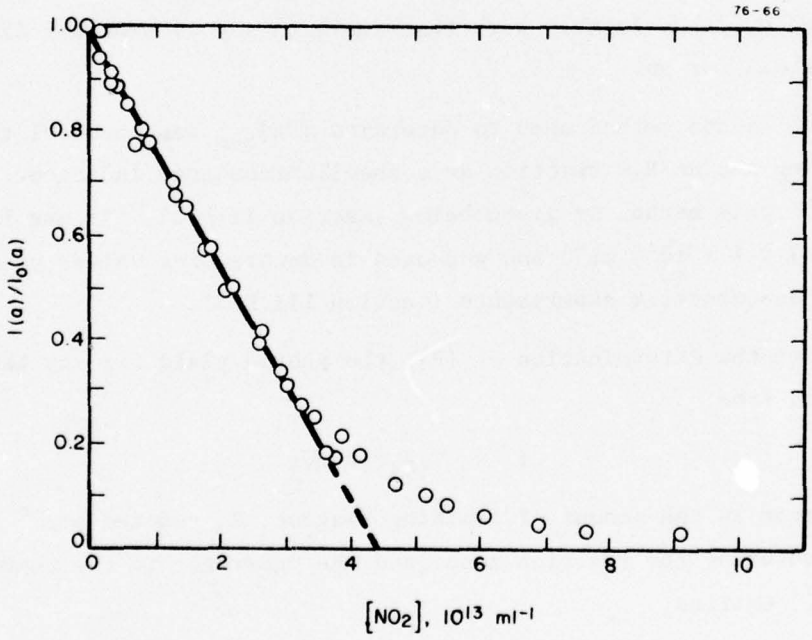

Figure 6. Results of titration of Sn with NO_2 using SnO(a—X) chemiluminescence as indicator. T = 895 K, [Ar] = 9.7×10^{16} ml^{-1} (9 torr), $\bar{v}$ = 48 m/sec, reaction time, t = 2.0 msec. Straight line represents extrapolation from initial linear portion of plot to endpoint, $[Sn]_o = (4.4 \pm 0.3) \times 10^{13}$ ml^{-1}.

Sn/NO_2 reaction were infinitely fast or if the reaction time were infinitely long such plots would be straight lines and their intercepts would equal the initial [Sn], $[Sn]_o$. In practice, neither of these conditions can be fulfilled; the range of applicability of these titration procedures was found to be limited in the present work to $[Sn]_o \geq 1 \times 10^{13}$ ml^{-1}. As $[Sn]_o$ increases above this value, extrapolations of the linear portions of curves such as figure 6 become progressively more accurate. In order to test the sensitivity of the titration procedure to possible errors in the extrapolation procedure, calculations of the shapes of titration curves under typical experimental conditions of the present work ($T \approx 900$, $\bar{v} \approx 50$ m/sec, $p \approx 10$ torr were made for $1 \times 10^{13} \leq [Sn]_o \leq 1 \times 10^{14}$ ml^{-1}; values for the rate coefficient, k_t, of the Sn/N_2O reaction were $3 \times 10^{-11} \leq k_t \leq 3 \times 10^{-10}$ ml molecule^{-1} sec^{-1}. This range of values was chosen as being larger than the probable range of values of k_t at 900 K (section III.A). The calculations indicate that the error in endpoint determination is always in the direction of overestimating $[Sn]_o$, and at worst (smallest k_t) ranges from $\approx$ 40% at $[Sn]_o = 1 \times 10^{13}$ ml^{-1} to < 1% at $[Sn]_o = 1 \times 10^{14}$ ml^{-1}.

The consistency and precision of the titration method were tested experimentally. To do this the Sn/N_2O chemiluminescence from both the short-lived $D^1\Pi - X^1\Sigma$ ($\tau_D \approx 10^{-5}$ sec) (ref. 2) and from the long-lived $a^3\Sigma - X^1\Sigma$ ($\tau_a \approx 1 \times 10^{-3}$ sec) (ref. 3) were used as indicators. Titrations using these indicators were performed for reaction times of 1.6 and 2.6 msec. A temperature of $\approx$ 1075 K was used in these experiments so that both these indicator emissions would be present with sufficient intensity for accurate measurement.† These measurements all extrapolated to the same ($\pm \approx 5\%$) value of $[Sn]_o$, indicating that the titration method is self-consistent to as good as $\approx \pm 5\%$. The NO_2 used in the titrations was prepared as a nominally 1% mixture in N_2 and analyzed using an AeroChem AA-2 Chemiluminescence Analyzer which showed $NO_2 = (0.91 \pm 0.02)\%$ and NO = 0.02% in the mixture.

---

† In actual experiments (at $T \leq 910$ K) only $a^3\Sigma$ emission could be used.

4. Quenching Rate Coefficient Measurements

Rate coefficients (or upper limits thereto) were measured for the quenching of the major emitters SnO ($a^3\Sigma$ and $A^3\Pi$) by Sn, N_2O, N_2, and Ar. Photon yields were obtained for the a–X and A–X emissions over a range of quencher concentrations. Rate coefficients were obtained from these data using the Stern-Volmer expression

$$\Phi_o/\Phi = 1 + \tau k_Q^X[X] \qquad (4)$$

where Φ_o and Φ are the photon yields for the a–X or A–X emission when X is absent and when X is present, respectively, τ is the radiative lifetime of the emitter, k_Q^X is the quenching rate coefficient, and [X] is the absolute quencher concentration.

For quenching measurements on reactant Sn, the experiments were arranged so that $[Sn]_o \geq 10[N_2O]$ ($[Sn]_o$ was measured by titration), thus making N_2O the limiting reagent. In these metal-in-excess experiments $[Sn]_{excess} \equiv ([Sn]_o - [N_2O])$ (ref. 21). Φ_o was obtained from oxidizer-in-excess measurements in which Sn was the limiting reagent i.e., Sn quenching was negligible, and in which $[Sn]_{abs}$ was determined from optical absorption measurements.

SECTION III

RESULTS

A. Sn/N_2O Overall Rate Coefficient

Results of measurements on the Sn/N_2O rate coefficient in the 300 to 1000 K range are summarized in table 1 and figure 7. These data indicate

$$k_1(T) = (1 \overset{\times}{\div} 4) \times 10^{-11} \exp(-(3000 \pm 1000)/T) \text{ ml molecule}^{-1} \text{ sec}^{-1}$$

over this range. The measurements at 300 K indicated a $k_1 < 10^{-15}$ ml molecule^{-1} sec^{-1}, which is consistent with an Arrhenius extrapolation of the present high

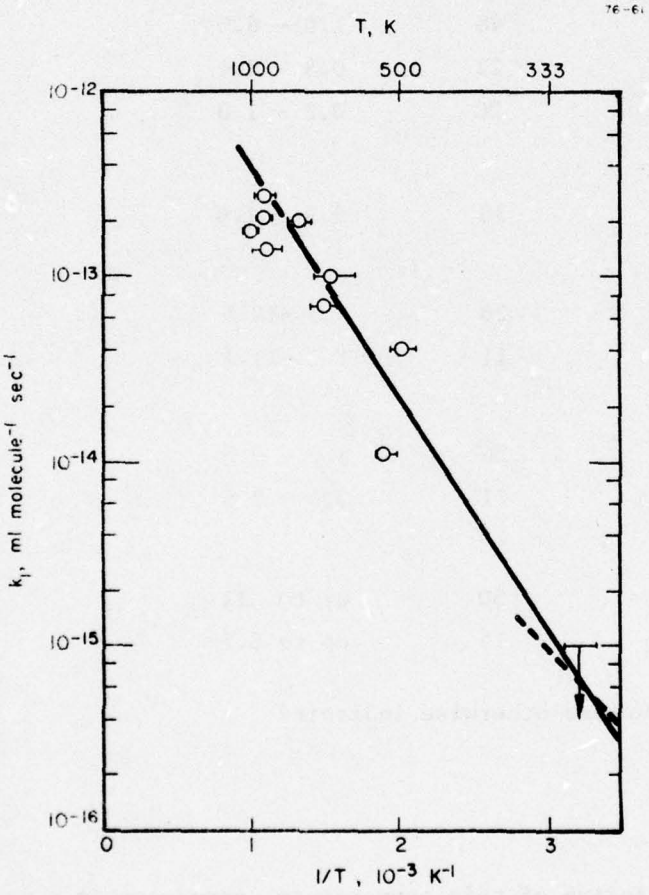

Figure 7. Arrhenius plot of Sn/N_2O rate coefficient measurements. Horizontal bars indicate range of temperatures in individual k_{ps_1} measurements. Measurements near 300 K gave upper limit shown. Measurements of reference 22 shown as dashed line.

temperature (T > 500 K, see fig. 7) results. These data are also in good agreement with the measurements of Wiesenfeld (ref. 22) who obtained, from 341 to 377 K: $k_1 = (5.0 \pm 1.0) \times 10^{-13} \exp(-(2000 \pm 100)/T)$. These latter results are shown in figure 7 as a dashed line.

Table 1

MEASUREMENTS OF Sn/N_2O OVERALL RATE COEFFICIENT

T (K)	p* (Torr)	$\bar{v}$ m/sec	$[N_2O]$ 10^{15} ml^{-1}	k_1 10^{-13} ml molecule^{-1} sec^{-1}
1000	10†	50	0.5 - 3.8	1.8
930	50†	48	1.0 - 6.0	1.4
930	38	22	0.3 - 2.4	2.1
910	10	20	0.2 - 1.0	2.7
745	10†	36	1.3 - 7.6	2.0
645	10	20	4.5 -12.5	1.0
669	40	11	1.7 -11.1	0.67
495	10	20	3.0 - 9.5	0.4
527	40	11	3.0 - 2.5	0.11
300	10†	50	up to 11	< 0.01
330	3†	15	up to 6.7	< 0.01

* N_2 bath gas unless otherwise indicated

† Ar bath gas

The finding of this temperature dependence is a major result of the present work, and has important advantages for the design of a laser device based on Sn/N_2O as further discussed in sections IV.A, C, and the Appendix. It may be seen from figure 7 that the >900 K data lie somewhat lower than the

Arrhenius plot would indicate, although certainly within the wide error limits of the fitting expression given above. In addition, the Sn/N_2O rate coefficient data we previously obtained (ref. 1) near 1000 K showed wide differences between stationary and traversing mode results. These facts suggest that N_2O decomposition is probably affecting these kinetic data at T > 900 K. Such decomposition must result from heterogeneous processes since the rate coefficient (ref. 23) for homogeneous gas-phase decomposition of N_2O is $8.3 \times 10^{-10} \exp(-29000/T)$ ml molecule^{-1} sec^{-1} which leads to destruction of only one N_2O molecule per 10^7 at 1000 K under the reaction conditions used. However, in equilibrium (which could rapidly be approached in heterogeneous reactions) over 90% of the N_2O is decomposed at 1000 K.† The present results, which apparently show a slight increase in $k_1(T)$ between 1000 K and 910 K suggest that the extent of decomposition is $\approx$ 50% to 70% near 1000 K and is rapidly decreasing to near zero by 900 K. Spectroscopic observations (section III.F) also indicate N_2O decomposition above 900 K.

B. Rate Coefficents for Reactions of $Sn(^3P_0, ^3P_1)$ with N_2O, NO_2 and O_2

As part of the effort to probe the mechanism of the Sn/N_2O reaction and in our search for a fast Sn titration reaction, we surveyed reactions of $Sn(^3P_1)$ with O_2 and N_2O, and of $Sn(^3P_0)$ with O_2 near 300 K and of $Sn(^3P_0)$ with NO_2 at near 300 K and 950 K. The results of these measurements, which cover a limited range of flow conditions are shown in table 2.

These measurements for $Sn(^3P_1)$ do not distinguish between physical and chemical quenching. The O_2 data agree very well with the results of ref. 24; this agreement further serves to increase our confidence in the low-temperature data obtained for the $Sn(^3P_0)/N_2O$ reaction (section III.A). An additional observation from these experiments is that it is not possible to observe $Sn(^3P_1)$ in N_2 bath gas at 300 K, while in Ar bath gas, sufficient $Sn(^3P_1)$ is obtained to allow kinetic measurements. This observation is con-

† Decomposition to even this extent does not affect the photon yield determinations (section III.C) since the minimum $[N_2O]/[Sn]$ used was $\approx$ 300 and typically was > 10^4. For measurements of N_2O quenching and Sn-quenching (metal-in-excess), reaction zone temperature was controlled to be < 920 K.

Table 2

RATE COEFFICIENTS FOR $Sn(^3P_J)$ REMOVAL BY VARIOUS OXIDIZERS

p* Torr	$\bar{v}$ m/sec	Oxidizer	T (K)	J	Present Results k, ml molecule^{-1} sec^{-1}	Reference 24 k, ml molecule^{-1} sec^{-1}
10†	50	N_2O	315	1	9×10^{-13}	
10	45	NO_2	950	0	4×10^{-10}	
10	34	NO_2	990	0	7×10^{-10}	
10	50	NO_2	315	0	4×10^{-13}	
3	15	NO_2	315	0	3×10^{-13}	
10	50	O_2	315	0	2×10^{-11}	3.5×10^{-11}
10†	50	O_2	315	0	2×10^{-11}	
3†	15	O_2	330	1	2×10^{-10}	8×10^{-11}

* N_2 bath gas unless otherwise indicated

† Ar bath gas

sistent with the larger N_2 quenching rate coefficient for $Sn(^3P_1)$ ($< 2.5 \times 10^{-13}$ ml molecule^{-1} sec^{-1}) (ref. 24) than that of Ar ($< 5 \times 10^{-16}$ ml molecule sec^{-1}) (ref. 24).

C. Photon Yield Determinations

Photon yield data from the Sn/N_2O reaction in N_2 (present work) and in Ar (present work and data of ref. 1) are summarized in tables 3 and 4, respectively. The major emissions may be seen to be the a–X and A–X band systems which will be discussed first.§ The data indicate that at $\approx 900 \leq T \leq 1000$ K,

§ The Φ data obtained in Ar in our preliminary work (ref. 1) ($T \approx 980$ K) have been normalized to the present Ar data (table 4) for all pressures above 10 torr because of poor absolute agreement. For p (Ar) < 10 torr, better agreement with the present results is obtained, and these data remain as previously (ref. 1).

Table 3

SnO PHOTON YIELD FROM [Sn] ABSORPTION MEASUREMENTS*
WITH N_2O IN EXCESS IN N_2

T (K)	$[N_2]$ 10^{17} ml^{-1}	p Torr	$[N_2O]$ 10^{15} ml^{-1}	Φ a–x	Φ A–X	Φ B–X	Φ D–X
900	11.8	110	5.0	0.50	0.13	---	---
920	11.8	110	4.8	0.52	0.12	---	---
920	11.8	112	2.5	0.48	0.12	0.04	0.03
890	6.3	58	4.7	0.52	0.16	---	---
915	6.3	60	5.1	0.50	0.14	---	---
920	3.1	30	4.8	0.52	0.15	---	---
907	1.6	15	10.5	0.50	0.17	---	---
909	1.6	15	7.0	0.55	0.18	---	---
907	1.6	15	5.1	0.46	0.16	---	---
920	1.6	15	1.9	0.48	0.16	0.05	0.01
920	1.6	15	1.9	0.51	0.16	0.06	0.01
916	1.6	15	1.8	0.56	0.16	---	---
907	1.6	15	1.2	0.48	0.16	---	---
909	1.6	15	0.73	0.53	0.15	---	---
907	1.6	15	0.51	0.47	0.16	---	---
920	1.6	15	0.05	0.51	0.16	---	---
930	0.5	4.5	2.8	0.24	0.10	0.07	0.02
675	9.7	68	5.0	0.36	0.12	<0.01	<0.01
660	2.2	15	5.0	0.42	0.10	<0.02	<0.01
510	2.5	13	5.0	0.47	0.04	<0.02	<0.01
300	1.0 - 4.8	3 - 15	up to 11	†	†	†	†

* $[Sn] \approx 10^{11}$ ml^{-1}

† No emission observed; Sn/N_2O reaction occurs at an immeasurably slow rate.

Table 4

SnO PHOTON YIELD IN Ar BATH GAS

T (K)	[Ar] 10^{17} ml^{-1}	p Torr	$[Sn]_o$ 10^{15} ml^{-1}	$[N_2O]_o$ 10^{15} ml^{-1}	Φ a–X	Φ A–X	Φ B–X	Φ D–X
885	10.9	100	2.0×10^{-4}	5.1	0.53	0.16	---	---
850*	6.8	60	1.6×10^{-4}	4.9	0.52	0.16	---	---
980†	4.9	50	1.5×10^{-4}	3.9	0.35(0.51)	0.10(0.15)	0.04	0.02
875	2.2	20	1.1×10^{-4}	4.8	0.51	0.15	---	---
1000†	1.0	10	3.1×10^{-4}	3.8	0.17(0.25)	0.09(0.13)	0.02	0.01
990†	1.0	10	2.1×10^{-4}	3.7	0.31(0.45)	0.15(0.22)	0.02	0.01
925	1.0	10	1.3×10^{-2}	1.3×10^{-3}	0.57	0.17	---	---
905	1.1	10	1.8×10^{-2}	1.7×10^{-3}	0.49	0.16	---	---
895	1.1	10	2.4×10^{-2}	2.9×10^{-3}	0.47	---	---	---
910	1.1	10	4.0×10^{-2}	3.5×10^{-3}	0.54	0.15	---	---
910	1.1	10	4.5×10^{-2}	4.0×10^{-3}	0.50	0.17	---	---
910	1.1	10	5.6×10^{-2}	5.5×10^{-3}	0.51	0.15	---	---
915	1.1	10	7.3×10^{-2}	3.4×10^{-3}	0.49	0.16	---	---
908	1.0	9.8	3.0×10^{-4}	5.0	0.51	0.16	---	---
880	1.0	8.8	4.2×10^{-4}	4.7	0.49	0.15	---	---
889	0.6	5.5	2.2×10^{-4}	4.1	0.52	0.06		
990	0.4	3.8	2.0×10^{-4}	3.2	0.12	0.07	0.02	0.01
1000	0.4	3.7	0.9×10^{-4}	3.1	0.07	0.06	0.01	0.007
660	2.2	15	1.8×10^{-4}	5.0	0.48	0.10	---	---

† For figure 9 these values have been normalized to the run marked by *. The normalizing constant, 1.46, is obtained from Φ(a, 60 torr)/Φ(a, 50 torr). Normalized values of Φ(a) and Φ(A) are given in parentheses.

and p ≥ 10 torr, Φ(a) = 0.51 ± σ = 6% in both N_2 and Ar and Φ(A) = 0.16 ± σ = 13% in Ar. In N_2, Φ(A) = 0.16 ± σ = 5% at 15 torr and decreases slightly thereafter (section III.D.2). The metal-in-excess values of Φ (for which only $[N_2O]$ enters into the calculation) will be seen to agree quite well with the Φ values for the oxidizer-in-excess which are based on [Sn] from absorption measurements. This agreement allows the overall accuracy of the photon yield measurements to be determined and, in so doing, the accuracy of the absorption-based measurements of $[Sn]_{abs}$ also to be assessed.

As indicated in section II.B.2, the Sn/N_2O glow in the metal-in-excess mode experiments extends beyond the range of traverse of the N_2O inlet. The $[Sn]_{excess}$ in the experiments is on the order of 3×10^{13} ml^{-1} (table 4)

which value will be used to illustrate the method of assessing the overall accuracy of the Φ and absorption-based [Sn] measurements. At this [Sn] the rate of reaction (1) is

$$-\frac{d\ \ln[N_2O]}{dt} = k_1[Sn] \approx 10\ sec^{-1}$$

at $\approx$ 900 K. Thus, in the $\approx 3 \times 10^{-3}$ sec time of reaction which is observed (22 cm reaction zone, 50 m/sec flow velocity), about 3% of the total reaction has taken place; the conclusions above are based upon observations of the chemiluminescence originating from that fraction of the reaction. In view of this, our usual procedure of extrapolation to obtain integrated intensity curves (figure 5 and section II.B.2) was supplemented by calculating the fraction of the total reaction observed in the HTFFR reaction zone, based on $k_1(910\ K) = 3.0 \times 10^{-13}$ ml molecule^{-1} sec^{-1} obtained from figure 7, and using the inverse of that fraction as the multiplier in equation 2 (section II.B.2). The agreement between these procedures was better than ± 25% in all cases, and better than ± 15% in seven of the eight metal-in-excess experiments made. This agreement between the two methods, one of which is completely determined by extrapolation of the observations and the other of which invokes the value of k_1 to calculate the fraction of reaction observed serves to increase our confidence in the present results.

In addition to this $\approx$ 20% uncertainty, the following error estimates are made: (i) the standard deviation of the Φ data--the 6% for $\Phi(a)$, 13% for $\Phi(A)$ in Ar, and 5% for $\Phi(A)$ in N_2 at 15 torr: these standard deviations are lumped together to obtain a rms standard deviation of 9% in Φ; (ii) $\approx$ 20% precision of the titration measurements to determine $[Sn]_o$ (section III.B.3); (iii) $\approx$ 20% lumped systematic uncertainties, and (iv) the 23% uncertainty in $\bar{v}$ (section II.B.1). Thus the accuracy of the Φ measurements, taken as the square root of the sum of the squares of the individual uncertainties is 42%, and we obtain, for $p \geq 10$ torr, $\approx 900 \leq T \leq 1000$ K

$$\Phi(a) = 0.51 \pm 0.22$$
$$\Phi(A) = 0.16 \pm 0.07$$

Table 4 shows excellent agreement (± 2%) between the Sn in excess and N_2O in excess Φ measurements. Since the former are based on knowledge of

the absolute value of $[N_2O]$, which is a routine measurement accurate to ± 5%, and the latter on the absorption based measurement of [Sn], it may be concluded that the accuracy of the absorption measurements, combining these error estimates as above, is 42%.

D. Pressure Dependence of $\Phi(a)$ and $\Phi(A)$

1. Low Pressure--The Possibility of a Precursor

$\Phi(a)$ and $\Phi(A)$ are apparently pressure dependent and this dependence is shown in figures 8 and 9. They rise to a maximum near 15 torr and thereafter remain constant or decrease slightly. Such an increase in Φ with p might suggest that, similar to the Ba/N_2O (refs. 21,25,26) and C_2O/O systems (ref. 27), the initial reaction results in the formation of precursor states which are collisionally transferred to radiating states. However, since the SnO (a and A) states have long radiative lifetimes ($\approx 10^{-3}$ and $> 10^{-5}$ sec, respectively)

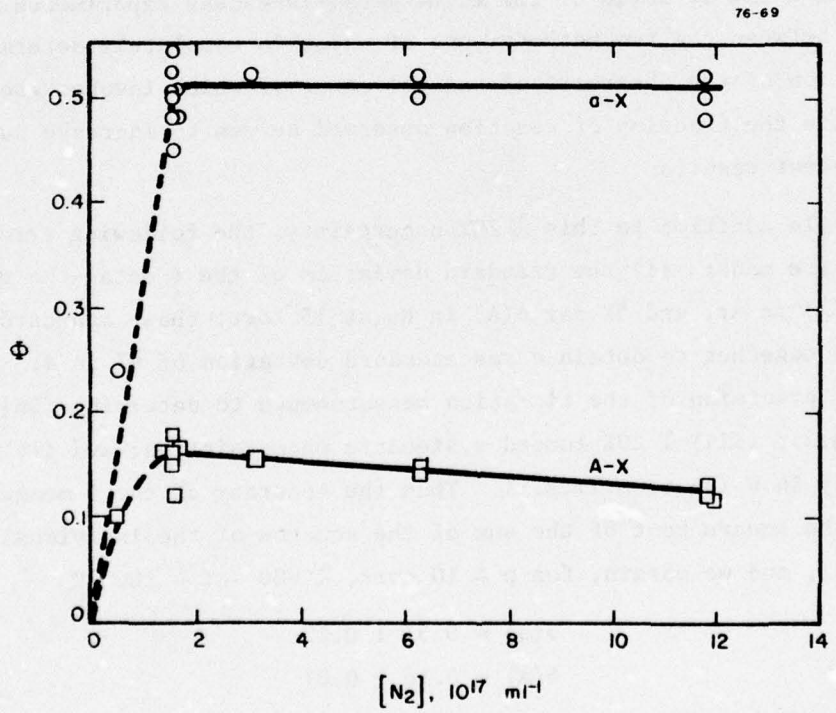

Figure 8. Absolute photon yields, $\Phi(a)$ and $\Phi(A)$, for Sn/N_2O chemiluminescence in the 900 to 1000 K range in N_2 bath gas. ○ - $\Phi(a)$, □ - $\Phi(A)$

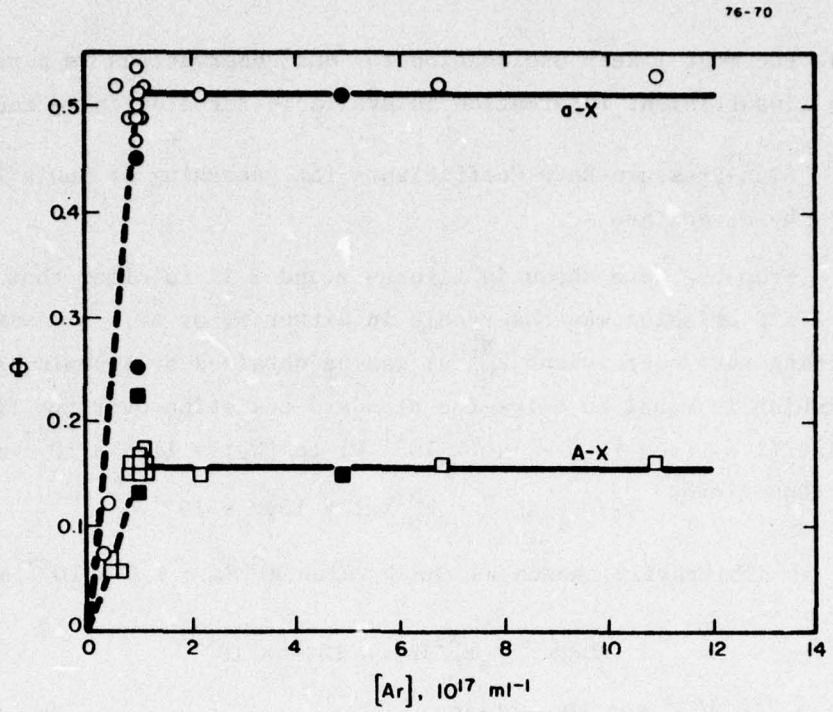

Figure 9. Absolute photon yields, $\Phi(a)$ and $\Phi(A)$, for Sn/N_2O chemiluminescence in the 900 to 1000 K range in Ar bath gas. ○ - $\Phi(a)$ present measurements; ● - $\Phi(a)$ measurements of reference 1 normalized to present results (see text); □ - $\Phi(A)$, present measurements; ■ - $\Phi(A)$, measurements of reference 1 normalized to present results (see text).

(refs. 3,15), it is possible that SnO(a and A) are formed directly in the attack step of reaction (1) and that at low pressures (< 15 torr) these molecules live long enough to diffuse to the reactor walls, there to be quenched; this process might well cause the observed apparent pressure dependence. Calculations on an idealized reactor using the Einstein relationship, $t = x^2/D$, where D (1000 K) $\approx$ 470cm^2/sec torr was calculated by the methods given in Reid and Sherwood (Ref. 28), yield an average diffusion time of SnO(a) to the HTFFR wall at 1000 K of 3 to 12 msec over the pressure range from $\approx$ 4 to 15 torr. In the actual reactor somewhat shorter times are probably effective due to obstacles such as the N_2O inlet. If τ_{rad} is indeed 10^{-3} sec then 95% of the SnO would radiate at 4 torr before collision with the wall, and the only interpretation for our data is the existence of a precursor mechanism. However if τ_{rad} were substantially longer, wall deactivation could be responsible for the observed pressure dependence.

Thus while the most likely explanation for our observations is a precursor mechanism, insufficient information is available for a definite conclusion.

2. High-Pressure-Rate Coefficients for Quenching of SnO($a^3\Sigma$ and $A^3\Pi$) by N_2 and Ar

From the data shown in figures 8 and 9 it is clear that no quenching of the $a^3\Sigma - X^1\Sigma$ emission was observable in either N_2 or Ar. A maximum value for the quenching rate coefficient $k_Q^{N_2}(a)$ can be obtained by assuming a slope in figure 8 which is equal to twice the standard deviation over the flat portion of the plot (i.e. from $[N_2] = 1.6 \times 10^{17}$ ml to $[N_2] = 11.8 \times 10^{17}$ ml^{-1}). Equation (4) then yields

$$\Phi_o/\Phi - 1 \geq \tau_a k_Q^{N_2}(a) \times 10.2 \times 10^{17}$$

where Φ_o is arbitrarily chosen as the Φ value at $[N_2] = 1.6 \times 10^{17}$ ml^{-1}

$$0.06 \geq \tau_a k_Q^{N_2}(a) \times 10.2 \times 10^{17}$$

Taking $\tau_a = 1 \times 10^{-3}$ sec, we obtain

$$k_Q^{N_2}(a) \leq 0.6 \times 10^{-16} \text{ ml molecule}^{-1} \text{ sec}^{-1}$$

Similar considerations for Ar yield

$$k_Q^{Ar}(a) \leq 1.0 \times 10^{-16} \text{ ml molecule}^{-1} \text{ sec}^{-1}$$

$\Phi(A)$ decreased with increasing N_2 (figure 8) from 0.16 at $[N_2] = 3.1 \times 10^{-17}$ ml^{-1} to 0.12 at $[N_2] = 11.8 \times 10^{17}$. To obtain $k_Q^{N_2}(A)$, we make the reasonable assumption that at $[N_2] \geq 3.1 \times 10^{17}$ ml^{-1} (30 torr) any precursor mechanism feeding into the $A^3\Pi$ state has reached its steady-state rate and/or that wall deactivation is negligible compared to radiation losses of SnO($A^3\Pi$). For these data equation (4) yields

$$\Phi_o(A)/\Phi(A) = 0.16/0.12 = 1 + \tau_A k_Q^{N_2}(A)\Delta[N_2]$$

where τ_A is the radiative lifetime of SnO($A^3\Pi$), and $\Delta[N_2] = (11.8 - 3.1) \times 10^{17}$ ml^{-1} (i.e. the range of $[N_2]$ for which the assumptions above are applied). $\Phi_o(A)$ and $\Phi(A)$ are the photon yields at the extremes of the $[N_2]$ range. We obtain

$$\tau_A k_Q^{N_2}(A) = 1.3 \times 10^{-18} \text{ ml molecule}^{-1}$$

This is as far as the analysis can be carried since the value of τ_A is even less well-known than τ_a.

Quenching of $SnO(A^3\Pi)$ by Ar is apparently negligible (figure 9). Applying the same arguments as above for $SnO(a^3\Sigma)$ quenching, we obtain

$$\tau_A k_Q^{Ar}(A) \leq 3.2 \times 10^{-19} \text{ ml molecule}^{-1}$$

E. Temperature Dependence of $\Phi(a)$ and $\Phi(A)$

The total photon yield only increases by a factor of $\approx$ 1.25 from 500 to 920 K, i.e. from 0.5 to 0.7. This increase is essentially all due to an increase in the A–X system intensity (Φ (A–X) increased from 0.04 to 0.16 over this range), while $\Phi(a–X)$ is nearly constant at $\approx$ 0.5. On the other hand, the rate constant for light emission, $k_{h\nu}$, defined by $d(h\nu)/dt = k_{h\nu}[Sn][N_2O]$, is a strong function of T since in addition, $k_{h\nu}(T) = k_1(T)\Phi(T)$ and $k_1(T)$ is temperature dependent. Thus, at 300 K, no emission is observed because $k_1(300)$ is so small, even though, e.g., $\Phi(a)$ is probably $\approx$ 0.5. Figure 10 shows a plot of $k_{h\nu}$ vs. 1/T for the a–X and A–X systems based on the value of $k_1(T)$ determined in section III.A, and the $\Phi(a)$ and $\Phi(A)$ values in tables 3 and 4.

F. Temperature and Pressure Dependence of $\Phi(B)$ and $\Phi(D)$

These observations were not a major goal of the present work but yield important information on the reaction mechanism. When the reactor temperature is raised significantly above 1000 K, a dramatic change in the Sn/N_2O chemiluminescence spectrum is observed. The a–X and A–X emissions decrease in intensity while the minor emissions increase. The spectral distribution at 1350 K is shown in figure 11 and may be compared to those obtained at 1000 K (ref. 1) and at 660 K (figure 12). Semiquantitative observations at 1200 and 1350 K show that in N_2 bath gas at 10 torr $\Phi(D) \approx 0.05$ and $\Phi(B) \approx 0.10$, i.e., the photon yields of these more than double from their 900-1000 K values (tables 3 and 4). Because of background radiation from the heated reactor walls at $T \geq 1200$ K, it was not possible to measure $\Phi(a)$ and $\Phi(A)$ quantitatively in these experiments. However by T = 1350 K, a–X and A–X emissions were completely undetectable although they would have easily (more than factor of 100 for a–X and 10 for A–X above the background radiation) been observed

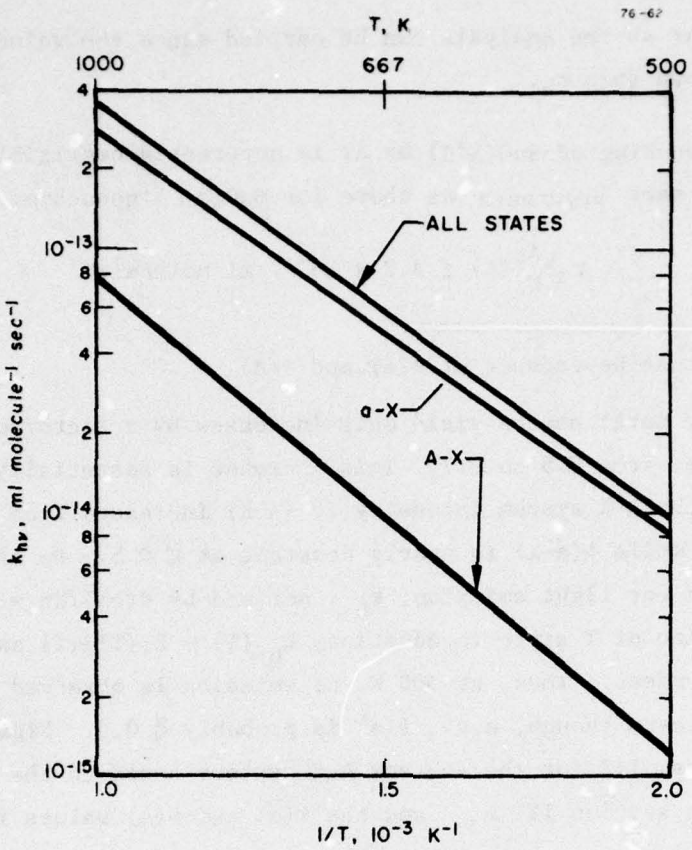

Figure 10. Temperature dependence of rate coefficient for light emission, $k_{h\nu}$, between 500 to 1000 K

if they had their 900-1000 K intensities. At 1350 K in equilibrium, decomposition of N_2O is essentially complete, which suggests that the B and D emissions do not arise directly from the Sn/N_2O reaction but more likely from the reaction Sn + O + M. The absence of a and A state emission from the 1350 K spectra rules out the possibility that either of these states is produced in a process which involves the B or D state. This argument implies that in the absence of O atoms, only a–X and A–X emissions should be observed. Our observations that $\Phi(B,D)$ are apparently absent at T < 900 K (tables 3,4 and figure 12) are consistent with these claims.

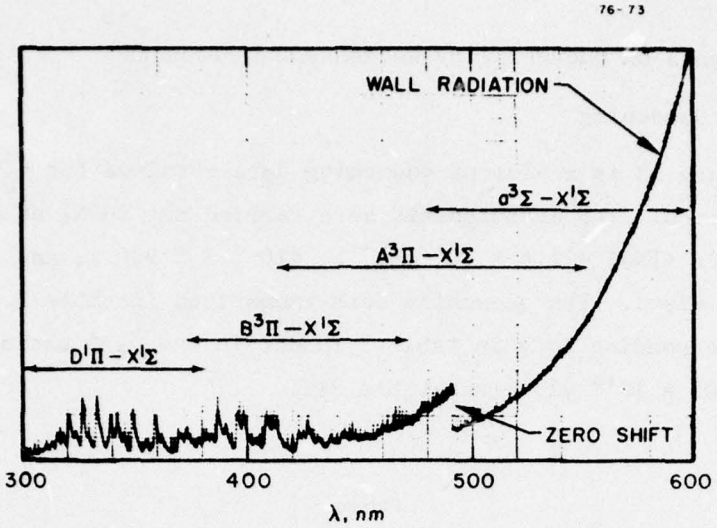

Figure 11. Spectrum (uncorrected for detector response) of Sn/N_2O chemiluminescence obtained at 1350 K. Note absence of a-X and A-X systems. $[Ar] = 1.4 \times 10^{17}$ ml^{-1} (20 torr), $\bar{v}$ = 25 m/sec, $[N_2O] = 3 \times 10^{15}$ ml^{-1}, $[Sn]_o = 5 \times 10^{11}$ ml^{-1}, t = 1.0 msec.

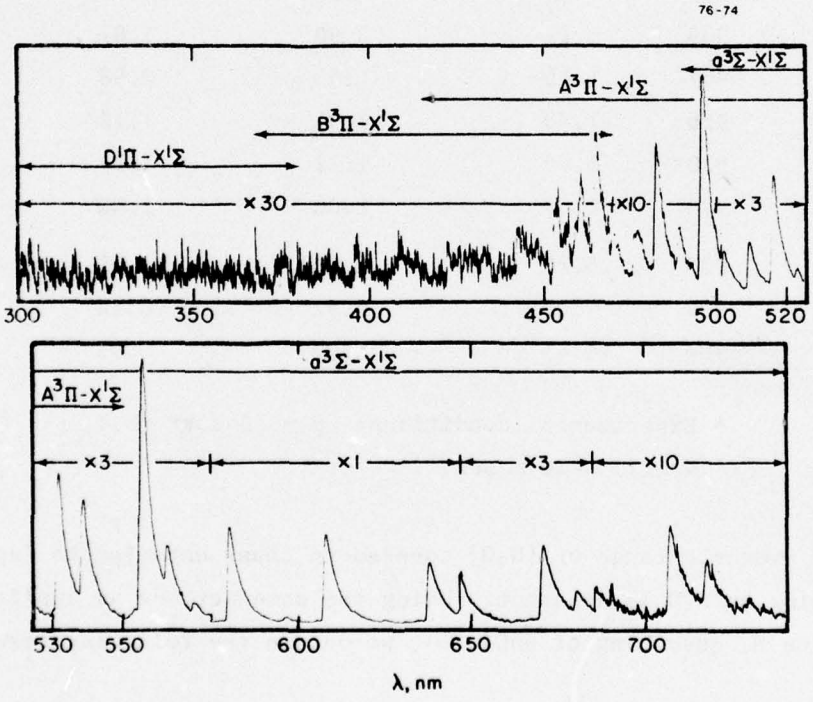

Figure 12. Spectrum of Sn/N_2O chemiluminescence (uncorrected for detector response) obtained at 660 K. Note apparent absence of D-X and B-X systems. $[Ar] = 1.6 \times 10^{17}$ ml^{-1} (11 torr), $\bar{v}$ = 28 m/sec, $[N_2O] = 4 \times 10^{15}$ ml^{-1}, $[Sn]_o = 2 \times 10^{11}$ ml^{-1}, t = 0.8 msec.

G. Measurements on Quenching by Reagents and Products

1. N_2O Quenching

Figure 13 is a plot of quenching data obtained for $k_Q^{N_2O}$ for the a–X and A–X emissions. The measurements were carried out in N_2 at a constant pressure of 15 torr ($[N_2] = 1.6 \times 10^{17}$ ml^{-1}), 910 ≤ T ≤ 920 K, and flow velocities from 13 to 30 m/sec. The quenching data summarized in table 5 were derived from the corresponding data in table 3 to obtain the Φ_o/Φ ratio. Φ_o was taken at $[N_2O] = 0.05 \times 10^{15}$ ml^{-1} (see table 3).

Table 5

N_2O QUENCHING* OF $SnO(a^3\Sigma)$ AND $SnO(A^3\Pi)$

T (K)	$[N_2O]$ 10^{15} ml^{-1}	$\Phi_o(a)/\Phi(a)$	$\Phi_o(A)/\Phi(A)$
920	0.05	1.00	1.00
907	0.51	1.08	0.98
909	0.73	0.96	1.07
907	1.15	1.06	0.98
916	1.80	0.91	1.13
920	1.89	1.12	1.10
920	1.89	1.00	1.00
907	5.10	1.12	1.01
909	7.02	0.92	0.88
907	10.45	1.02	0.93

* Experimental conditions: p = 15 torr (N_2), $\bar{v}$ = 13 to 30 m/sec.

Over the range of $[N_2O]$ covered in these experiments (up to 1 torr), no quenching by N_2O is apparent. Using the same methods as applied to analyze the data on N_2 quenching of $SnO(a^3\Sigma)$, we obtain the following results.

$$k_Q^{N_2O}(a) \leq 1 \times 10^{-14} \text{ ml molecule}^{-1} \text{ sec}^{-1}$$

(for $\tau_a = 1 \times 10^{-3}$ sec) and

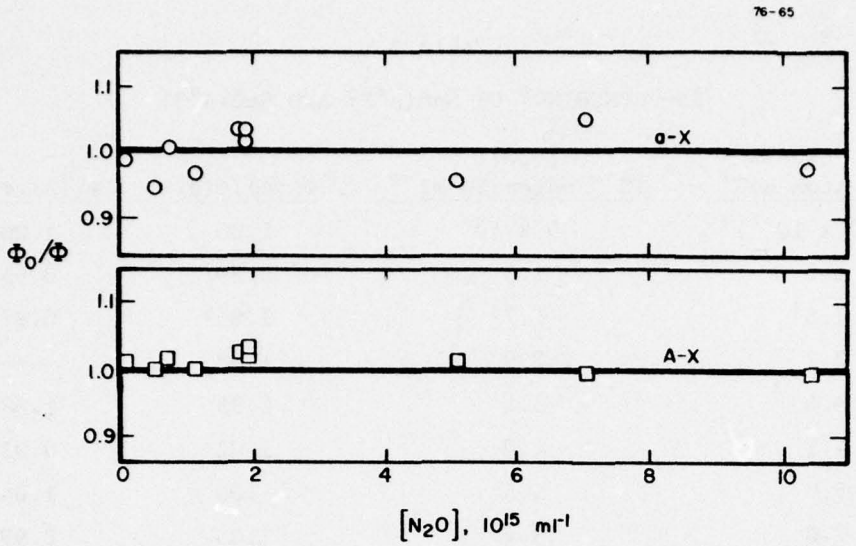

Figure 13. Influence of $[N_2O]$ on relative photon yields of SnO(a-X and A-X) chemiluminescence from Sn/N_2O reaction. T = 920 K, $[N_2]$ = 1.6 × 10^{17} ml^{-1} (15 torr), $\bar{v}$ = 13 to 30 m/sec, 2 × 10^{11} ≤ $[Sn]_o$ ≤ 5 × 10^{11} ml^{-1}.

$$\tau_A k_Q^{N_2O}(A) \leq 1.4 \times 10^{-17} \text{ ml molecule}^{-1}$$

2. Sn Quenching

Measurements of Sn quenching were carried out using the metal-in-excess method. The Φ_o/Φ values are displayed in table 6 and figure 14. Φ_o was determined at $[N_2O]$ = 5.0 × 10^{15} ml^{-1}, p (Ar) = 9.8 Torr and [Sn] = 3×10^{11} ml^{-1} as measured in absorption (see table 4); Φ values were determined at [Sn]> 1 × 10^{13} ml^{-1} as measured by titration. It will be recalled that the data are based on observations of the initial portion of the chemiluminescence glow and that two methods for obtaining integrated intensity (extrapolation and calculation), which agreed within ≈ 20% were used (section III.C). The data indicate no significant Sn-quenching of $SnO(a^3\Sigma)$. As a first estimate of $k_Q^{Sn}(a)$ and $\tau_A k_Q^{Sn}(A)$ we use the mean and standard deviation of the data in table 1. Apply-

Table 6

Sn-QUENCHING* OF $SnO(a^3\Sigma)$ AND $SnO(A^3\Pi)$

$[Sn]_{excess}$ 10^{13} atom ml^{-1}	$[N_2O]$ 10^{12} molecule ml^{-1}	$\Phi_o(a)/\Phi(a)$	$\Phi_o(A)/\Phi(A)$
(3.0×10^{-2})†	5×10^3	1.00	1.00
1.2	1.3	0.89	0.94
1.6§	1.7§	1.05§	0.97§
2.2	2.9	1.08	---
3.6	3.5	0.95	1.08
4.1	4.0	1.02	0.93
5.0	5.5	1.00	1.04
7.0	3.4	1.05	0.99
	Mean and std. deviation:	$1.00_5 \pm 0.06_1$	$0.99_3 \pm 0.05_3$

* Experimental conditions: T = 910 ± 15 K, p = 10 torr (Ar)

† Determined from line absorption measurements

§ $\bar{v}$ = 22 m/sec; in all other experiments $\bar{v}$ = 48 m/sec

ing Student's t-test (ref. 29)' we find that the 95% confidence interval (selected as a conservative interval) is given by $\Phi_o(a)/\Phi(a) = 1.00_5 \pm 0.05_1$ and $\Phi_o(A)/\Phi(A) = 0.99_3 \pm 0.04_1$; we are thus 95% certain that the value of $\Phi_o(a)/\Phi(a)$ changes by no more than 0.10_3 and the value of $\Phi_o(A)/\Phi(A)$ by no more than 0.08_2 (i.e. by no more than the difference between the extremes of

† The data treatment for these results was more extensive than for other quenchers because of the importance of Sn-quenching and the relatively smaller range of [Sn] which could be achieved in these experiments. A larger range of [Sn] would be accessible with extensive HTFFR modifications, but such modifications were not possible within the scope of the present work.

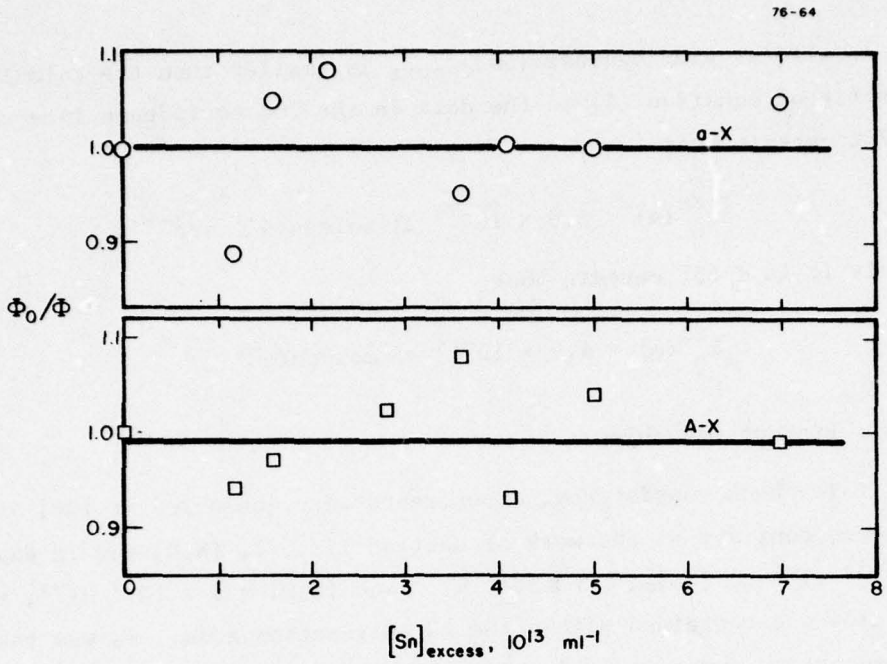

Figure 14. Influence of $[Sn]_{excess}$ on relative photon yields of SnO(a-X and A-X) chemiluminescence from Sn/N_2O reaction. $900 \leq T \leq 920$ K, $[Ar] = 1.0 \times 10^{16}$ ml^{-1} (9 torr), $\bar{v} = 50$ m/sec.

the confidence intervals) in the range of $[Sn]_{excess}$ covered. From these upper limits, equation (4) and the largest $[Sn]_{excess}$ ($= 7 \times 10^{13}$ ml^{-1}) used we calculate†

$$k_Q^{Sn}(a) < 1.5 \times 10^{-12} \text{ ml molecule}^{-1} \text{ sec}^{-1}$$

$$\tau_A k_Q^{Sn}(A) < 1.3 \times 10^{-15} \text{ ml molecule}^{-1}$$

The data of table 6 were also directly tested for the existence of trends, i.e. slopes in plots of the relative photon yields against $[Sn]_{excess}$, using methods based on the analysis of variance (ref. 29). These tests show that the slope

† The error introduced by possible overestimation of $[Sn]_o$ in titration (section II.B.2) is negligible (< 3%) at this large $[Sn]_o$ and was thus neglected here.

of the $\Phi_o(a)/\Phi(a)$ plot against $[Sn]_{excess}$ is smaller than the calculated least squares fit of equation (4) to the data in the 70% confidence interval, i.e. it is 70% certain that

$$k_Q^{Sn}(a) < 6.5 \times 10^{-13} \text{ ml molecule}^{-1} \text{ sec}^{-1}$$

Similarly it is $\tilde{\approx}$ 65% certain that

$$\tau_A k_Q^{Sn}(A) < 4.9 \times 10^{-16} \text{ ml molecule}^{-1}$$

3. Product Quenching

To check consistency, experiments were conducted at $[Sn] > 1 \times 10^{13}$ ml^{-1} where, contrary to the work of section III.G.2, $[N_2O]$ was in excess. For 2.2×10^{13} $ml^{-1} \leq [Sn]_o \leq 4.5 \times 10^{13}$ ml^{-1} and $[N_2O] = 5 \times 10^{15}$ ml^{-1}, the entire Sn/N_2O glow was contained within the 20 cm reaction zone. Φ_o was taken, as in the Sn-quenching experiments (section III.G.2) with $[Sn]_o = 3 \times 10^{11}$ ml^{-1}. The results of these measurements are displayed in table 7 and figure 15.

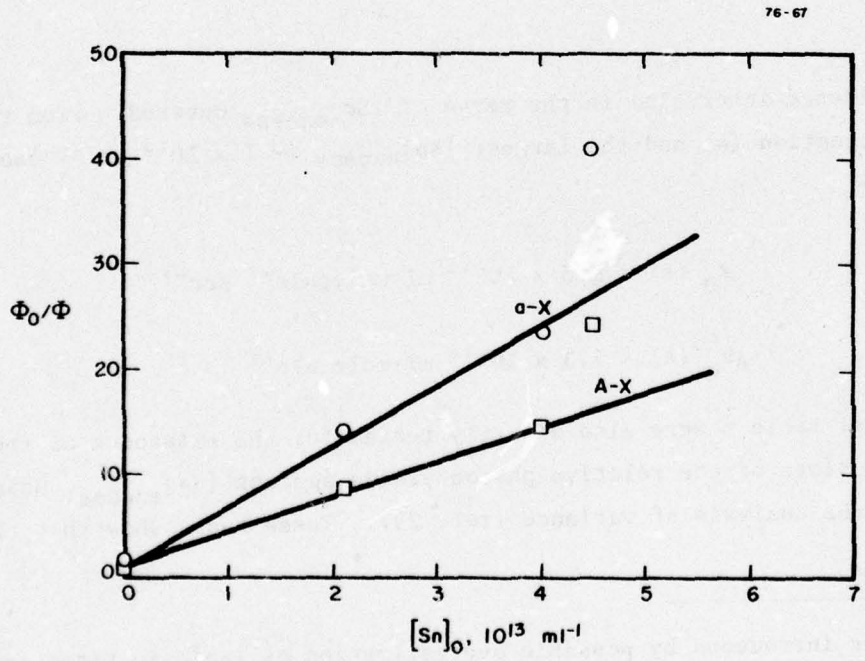

Figure 15. Influence of reaction products on relative photon yields of SnO(a-X and A-X) chemiluminescence from Sn/N_2O reaction. T = 920 K, $[Ar] = 1.0 \times 10^{16}$ ml^{-1} (9 torr), $\bar{v}$ = 50 m/sec.

Table 7

PRODUCT QUENCHING* OF $SnO(a^3\Sigma)$ AND $SnO(A^3\Pi)$

$[Sn]_o$ 10^{13} atom ml^{-1}	$\Phi_o(a)/\Phi(a)$	$\Phi_o(A)/\Phi(A)$
$(3 \times 10^{-2})^\dagger$	1.00	1.00
2.2	13.9	8.5
4.1	24.5	14.5
4.5	41.0	24.1

* Experimental conditions: T = 905 ± 15 K, p = 10 torr (Ar), $\bar{v}$ = 50 ± 2 m/sec, $[N_2O] = 5 \times 10^{15}$ ml^{-1}

† Determined from line absorption measurements

These data display a marked quenching effect. Since the results obtained up to this point indicate negligible reagent (Sn or N_2O) and bath gas (Ar) quenching, this effect is most likely due to the reaction products. To interpret the data of figure 15 and to obtain upper limits to the magnitudes of the product quenching rate coefficients, we take as a first approximation that the quencher concentration $[X] = [Sn]_o$. From the slopes of the lines, we then obtain (taking $\tau_a = 1 \times 10^{-3}$ sec)

$$k_Q^X(a) \approx 5 \times 10^{-10} \text{ ml molecule}^{-1} \text{ sec}^{-1}$$

and

$$\tau_A k_Q^X \approx 3 \times 10^{-13} \text{ ml molecule}^{-1}$$

These values are based upon only three observations and must be considered as preliminary. Since product quenching could represent a potentially serious obstacle to the realization of an Sn/N_2O based chemical laser it is necessary to examine the available data to try to determine the identity of the quencher. From the examination, which follows, two important conclusions may be drawn:

(i) The identity of the quencher is probably not SnO.

(ii) Based on (i) the observed quenching effect will probably not be an important limitation of an Sn/N_2O based chemical laser.

In the titration experiments the indicator chemiluminescence originates under nearly identical experimental conditions of $[Sn]_o > 1 \times 10^{13}$ ml^{-1}, $[N_2O] \geq 1 \times 10^{15}$ ml^{-1}, p = 10 torr, $\bar{v}$ = 50 m/sec, as those used in the present series of measurements given in table 7 and figure 15. (The major difference is that in the titration experiments the indicator reagent (N_2O) inlet is not traversed.) Thus we can examine that glow to obtain information on the identity of the quenchant. If the quenchant were SnO(X):

$$\begin{aligned} Sn + N_2O &\rightarrow SnO(a) + N_2 && k_1\Phi(a) \\ SnO(X) + SnO(a) &\rightarrow \text{products} && k_Q^X(a) \\ SnO(a) &\rightarrow SnO(X) + h\nu_a && 1/\tau_a \end{aligned}$$

and the amounts of Sn and SnO(X) in the indicator reaction region are determined by the amount of titrant (NO_2) added†, i.e.:

$$\begin{aligned} [Sn] &= [Sn]_o\,(1 - [NO_2]/[Sn]_o) \\ [SnO(X)] &= [NO_2] \end{aligned}$$

where $[Sn]_o$ is [Sn] before the addition of a flow of titrant and [Sn] and [SnO(X)] are the concentrations arriving at the indicator reaction region. $[NO_2]$ is calculated from the flow of NO_2 into the HTFFR (section II.B.3).

From these kinetic equations we obtain, as a first approximation, the steady-state indicator chemiluminescence intensity§

$$I(a) = k_1\Phi(a)[Sn]_o[N_2O](1 - [NO_2]/[Sn]_o)/(1 + \tau_a k_Q^X(a)[NO_2])$$

---

† The titration reaction, $Sn + NO_2 \rightarrow SnO(X) + NO$, is assumed to have gone essentially to completion. For simplicity, SnO(X) formed in the Sn/N_2O reaction is ignored. Its inclusion in this treatment would serve to enhance the quenching effect on indicator chemiluminescence.

§ The steady-state assumption is not strictly valid here since the entire indicator chemiluminescence is not observed; however, since $[N_2O] >> [Sn]$, and the peak of the spatial distribution of the indicator chemiluminescence (cf. figure 5) was always observed, the steady-state assumption should yield qualitatively correct results.

where the substitution $[SnO(a)]/\tau_a = I(a)$ has been used. The chemiluminescence intensity when no titrant is added is

$$I_o(a) = k_1\Phi(a)[Sn]_o[N_2O]$$

Hence, the titration curves in which SnO(X) quenching of SnO(a) has an effect would have the functional form

$$I(a)/I_o(a) = (1 - [NO_2]/[Sn]_o)/(1 + \tau_a k_Q^X(a)[NO_2]) \qquad (5)$$

Similar considerations for the other assumed product quenchers SnO(a) and SnO(A), lead to more complicated expressions, e.g., for SnO(a) (the identical expression is obtained for SnO(A)):

$$I(a)/I_o(a) = \left[1 + \left\{1 + 4\tau_a{}^2 k_1 \Phi(a)[Sn]_o[N_2O](1 - [NO_2]/[Sn]_o)k_Q^a(a)\right\}^{1/2}\right] \Big/ \left[1 + \left\{1 + 4\tau_a{}^2 k_1\Phi(a)[Sn]_o[N_2O]k_Q^a(a)\right\}^{1/2}\right] \qquad (6)$$

Equations (5) and (6) were numerically evaluated as functions of $[NO_2]$ for typical experimental conditions (e.g., $[Sn]_o = 3 \times 10^{13}$ ml^{-1}, $[N_2O] = 3 \times 10^{15}$ ml^{-1} with $\tau_a = 1 \times 10^{-3}$ sec and taking $k_Q^X(a) = k_Q^a(a) = 3 \times 10^{-10}$ ml molecule^{-1} sec^{-1}) in order to compare with experimentally observed titration plots.

The calculated curves do not agree well with the observed titration curves, as shown in figure 16. In this figure, titration curves have been plotted for both product quenching cases and for the case of no product quenching; for comparison the results of an actual titration are superimposed on the plot. From a consideration of these plots we can conclude that the identity of the major quencher is not likely to be SnO(any state) since such a large quenching effect, as indicated by figure 15, would have been apparent in the titration measurements.

If the product quencher is not, as the foregoing arguments suggest, ground state or excited SnO, then the prospect that this observed product quenching will not be important in a chemical laser can be demonstrated as follows. For if SnO does not quench itself, and since N_2O, N_2 (and Ar and Sn) do not quench SnO(a) significantly under the conditions of these experiments, the quenching must be due to a secondary product, e.g., SnO_2 from reactions of SnO

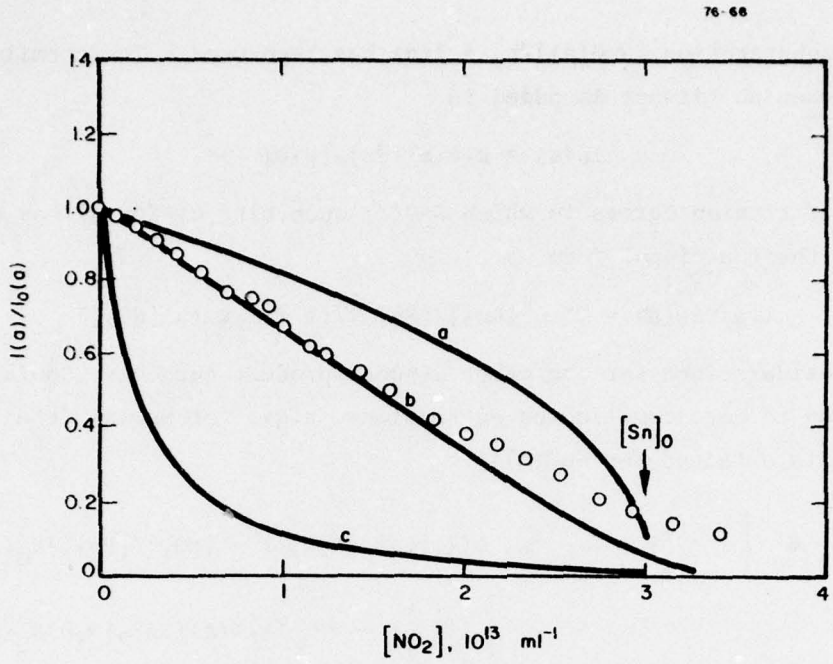

Figure 16. Calculated titration curves showing effect of significant $SnO(a^3\Sigma^+)$ quenching by reaction products. Curve (a) - quenching of SnO(a) by SnO(a); Curve (b) - no quenching; Curve (c) - quenching of SnO(a) by SnO(X); o - results of actual titration measurement: T = 910 K, $[Sn]_o = 3.0 \times 10^{13}$ ml^{-1}, $[Ar] = 1.0 \times 10^{16}$ ml^{-1} (9 torr), $\bar{v}$ = 48 m/sec.

with N_2O or particles which might form under these 'high' $[N_2O]$ and [Sn] conditions. Whatever the actual identity of a quencher formed as a secondary product, the time scale of such a process would probably make it possible to prevent its occurrence in the region of gain by, e.g., using high flow velocities in a practical laser device. In the present experiments, the quenching by such a secondary product competes with the long natural radiative lifetime as a loss process for SnO(a); in a laser device, the stimulated lifetime would be much shorter than τ_a, and SnO(a) would be used up by stimulated emission before a secondary product (quencher) could form in sufficient concentration to interfere. If the quenching agent in the present measurements forms simply as an artifact of the experiment, then it probably will not be a problem in a practical laser device which will differ both in design and operation from an HTFFR.

The preceding arguments suggest that the large observed product quenching rate coefficients may not seriously jeopardize the operation of an Sn/N_2O based chemical laser. The need now is to obtain sufficient experimental data to verify these promising conclusions, e.g., to confirm the present scant product quenching data under a variety of experimental conditions and to identify the quenching agent and elucidate the kinetics of its formation and destruction.

SECTION IV

GENERAL DISCUSSION AND CONCLUSIONS

A. Photon Yields and the Feasibility of an Sn/N_2O-Based Chemical Laser

The observed value of $\Phi(a) = 0.51 \pm 0.22$ (section III.C.) is to be compared with those obtained by Linevsky and Carabetta (ref. 15) and Capelle (ref.30). These investigators obtain $\Phi(a) \gtrsim 0.003$ (ref. 15) and < 0.01 (ref. 30). It appears that these discrepancies with our results, as well as the intense B–X and D–X emissions observed in the work of Linevsky and Carabetta (ref. 15) can be rationalized in terms of four factors: (i) incomplete Sn consumption in their systems, (ii) the temperature dependence of k_1, (iii) the occurrence of the Sn + O + M reaction at high temperatures and (iv) the possibility of a large product-quenching rate coefficient. The first two of these factors offer an apparent explanation for the low photon yield obtained by Capelle (ref. 30). His experiments were carried out in a diffusion flame apparatus, in which T may be estimated to be only $\lesssim$ 400 K. At this temperature, the Sn/N_2O reaction is too slow to consume all Sn present in the observation zone, hence leading to an apparent low Φ. Factors (i), (iii) and (iv) can contribute to the observations of Linevsky and Carabetta (ref.15). In these experiments, the use of H_2/N_2O flames produces copious quantities of O atoms and the occurrence of the Sn + O + M reaction cannot be neglected in the determination of Φ. In addition, the calculated (from SnO $X^1\Sigma^+ \rightarrow D^1\Pi$ absorption measurements) concentration (ref. 15) of SnO(X) in the flame is $\gtrsim 10^{13}$ $ml^{-1} \leq [SnO(X)] \leq 2 \times 10^{14}$ ml^{-1}, at which concentration, secondary reactions leading to quenching could also be responsible for the apparent low Φ. Linevsky and Carabetta also observed metallic Sn deposits on their apparatus surfaces, indicating that Sn consumption was not complete. Such an effect would also result in an underestimate of Φ.† We conclude that the present HTFFR measurements of Φ, by being carried out under conditions of independently controlled temperature, pressure and reagent concentrations and in a simpler chemical environment than the measurements of reference 15, represent the better determination of photon yield from the Sn/N_2O reaction.

---

† In a recent pulsed shock tube $Sn(CH_3)_4/N_2O$ experiment at SRI (ref. 31) low $\Phi(a)$ and strong D emission were observed. We have not seen details of this experiment but the D emission again suggests N_2O dissociation as the cause of the low $\Phi(a)$.

Based on $\Phi(a) = 0.51$, the feasibility of obtaining gain on $SnO(a^3\Sigma - X^1\Sigma)$ transitions in an Sn/N_2O based laser is calculated, assuming that quenching of $SnO(a^3\Sigma)$ is negligible. The method employed in these calculations is given in the Appendix, and is based on the work of references 32 and 33. These calculations (i) show that gain is achievable and (ii) give estimates for the densities of SnO or equivalently Sn, needed to achieve reasonable gains of, e.g., $\tilde{>}$ 0.1% cm^{-1}. The experimental situation envisioned is one in which Sn and N_2O are premixed at a low temperature taking advantage of the T-dependence of k_1 (section III.a) and are then reacted in a flow transverse to an optical axis, with complete reaction occuring just prior to the passage of the mixture across the axis. Then, in the absence of quenching or radiative relaxation,

$$[SnO(a^3\Sigma)] = 0.5[Sn]_o$$

and

$$[SnO(X^1\Sigma)] = (1-0.7)\,[Sn]_o = 0.3[Sn]_o \,^{\dagger}$$

where $[Sn]_o$ is the Sn concentration prior to reaction with (an excess of) N_2O in the (constant density) flow. To evaluate the gain equation (Appendix, eq. A-1), τ_a is taken to be 1×10^{-3} sec, and the Honl-London factors $S(J', J'')$, are assumed, for the purpose of these calculations to be well-enough approximated (ref. 32) by J' and the vibrational-rotational distributions for $a^3\Sigma$ and $X^1\Sigma$ are Boltzmann at the bath gas T (Appendix). The ratio involving the product of the electronic moments and the Franck-Condon factors and their sum is taken to be 0.2.[§] Values used for ν are those given by Linevsky (ref. 15), i.e., $\nu = \nu_{oo} + 499\,v' - 819\,v''$. For a temperature of 1000 K, the equation for gain (eq. A-1, Appendix) becomes

$$\gamma = 1.8 \times 10^{-7} \frac{J'}{\nu^3} [Sn]_o \; 0.34 \exp[-(4.04 \times 10^{-4})\, J'(J'+1)] \times \exp(-0.72\, v') - 2.3 \exp[-(5.2 \times 10^{-4})\, J''(J''+1)] \times \exp(-1.18\, v'')$$

Maximum gain will be exhibited (ref. 32) by states with $J' \tilde{>} (kT/2hB)^{1/2} = 35$.

---

† We have assumed $\Phi_{TOT} = 0.7$, i.e. a 3% contribution from the B and D states.

§ From the appearance of the $a^3\Sigma \rightarrow X^1\Sigma$ spectrum, this approximation probably results in underestimation of gain for $v'' = 2, 3$ and 4 and overestimation for $v'' \geq 5$.

Table 8 gives samples of values for γ per Sn atom entering the reaction region. It can be seen that, if $[Sn]_o = 1 \times 10^{16}$ ml^{-1}, gains approaching 0.3% cm^{-1} are obtained for $v'' \geq 2$ and $v' = 0$ on the R-branch for $J' = 35$.

Table 8

SAMPLE GAIN CALCULATION RESULTS FOR $SnO(a^3\Sigma - X^1\Sigma)$

Bandhead Wavelength* nm	v'	v''	J'	J''	$\gamma[Sn]_o^{-1}$ cm^{-1} ml molecule^{-1}
488.0	0	0	35	36	-0.7×10^{-19}
508.2	0	1	35	36	-1.2×10^{-19}
530.0	0	2	35	36	0.9×10^{-19}
553.5	0	3	35	36	1.8×10^{-19}
578.8	0	4	35	36	2.4×10^{-19}
606.4	0	5	35	36	2.9×10^{-19}

* From reference 15.

B. Quenching of $SnO(a^3\Sigma$ and $A^3\Pi)$

The rate coefficients (or upper limits thereto) obtained in the present work are summarized in table 9. The data presented are based on an assumed radiative lifetime of 1×10^{-3} sec^{-1} for $SnO(a^3\Sigma)$ which is intermediate between the upper and lower limits. The value of τ_A is even less well-known, and the values reported in table 9 are therefore Stern-Volmer slopes, $\tau_a k_Q^X(A)$. As can be seen from these results, quenching by bath gases N_2 and Ar is negligible for $SnO(a^3\Sigma)$. $SnO(A^3\Pi)$ is slightly deactivated by N_2 and is unaffected by Ar.

Quenching by reagents N_2O and Sn likewise is negligible over the range of concentrations covered. The largest concentration of $[N_2O]$ which could be used in this work was $\approx 1.0 \times 10^{16}$ ml^{-1} which corresponds to a pressure of ≈ 1 torr at 910 K where the N_2O quenching experiments were carried out. Under the experimental conditions used, this amount of N_2O constituted about 10% of the total gas flow through the HTFFR. This percentage is the maximum we have found to be useful in providing kinetic data, since introducing larger

Table 9

QUENCHING RATE COEFFICIENTS, k_Q, FOR SnO($a^3\Sigma$ AND $A^3\Pi$)

Quencher	$k_Q(a)$* ml molecule^{-1} sec^{-1}	$\tau_A k_Q(A)$ ml molecule^{-1}
N_2	$\leq 0.6 \times 10^{-16}$	1.3×10^{-18}
Ar	$\leq 1.0 \times 10^{-16}$	$\leq 3.2 \times 10^{-19}$
N_2O	$\leq 1.0 \times 10^{-14}$	$\leq 1.4 \times 10^{-17}$
Sn	$\leq 1.2 \times 10^{-12}$	$\leq 1.3 \times 10^{-15}$
"Product"	5×10^{-10}	3×10^{-13}

* Assumed that $\tau_a = 1 \times 10^{-3}$ sec

flows through the inlet ring causes large flow disturbance and interferes with accurate measurements. In order to reduce the upper limit values for the $k_Q^{N_2O}$ obtained, it would be necessary to introduce additional N_2O, e.g., by mixing with part of the room temperature bath gas introduced in the temperature transition zone of the modular HTFFR (section II.A). The presently obtained upper limits to the $k_Q^{N_2O}$ values are sufficiently low that N_2O quenching would not reduce SnO($a^3\Sigma$) by more than $\tilde{\sim}$ 1% of its initial value in an operational laser device of the kind suggested in section IV.A. We conclude that the present determination of the $k_Q^{N_2O}$ is sufficient to indicate that N_2O quenching is negligible in the context of chemical laser application.

The presently obtained upper limit to N_2O quenching of SnO($a^3\Sigma$) ($k_Q^{N_2O}(a) \leq 1 \times 10^{-14}$ ml molecule^{-1} sec^{-1}) is about three times smaller than the value obtained by Linevsky and Carabetta (ref. 15) from their Sn-containing flame ($k_Q^{N_2O}(a) = 3.3 \times 10^{-13}$ ml molecule^{-1} sec^{-1} with $\tau_a = 1 \times 10^{-3}$ sec). We are not certain of the origin of this discrepancy at present. However, it should be pointed out that the inferred value of $k_Q^{N_2O}$ in their work depends upon assuming an up to eleven-step mechanism for the observed flame emissions (ref. 15), whereas the present result is based simply upon observations of intensity loss. The present results on N_2O quenching were obtained at constant p, $\bar{v}$, and $\bar{T}$, and therefore are not subject to systematic variations due to possible changes in reaction mechanism, which might arise under changing reaction conditions.

The results on Sn quenching are similarly encouraging for chemical laser application. The upper limit obtained for $k_Q^{Sn}(a)$ in these studies is sufficient to indicate that Sn quenching would not reduce [$SnO(a^3\Sigma)$] by more than about 10% of its initial value in the laser device suggested in the previous section. This reduction is about the largest which might be considered acceptable from quenching losses in an operating device. Of course, the present value of $k_Q^{Sn}(a)$ is an upper limit, and further experiments at higher $[Sn]_{excess}$ than used in this work should be carried out to reduce this upper limit or to obtain values for $k_Q^{Sn}(a)$ and $\tau_A k_Q^{Sn}(A)$.

The inefficiency of Sn in quenching SnO(a,A) may be explained on the basis of energy-level considerations. Only two low-lying Sn states, ^1S and ^1D, are energetically accessible (ref. 11) via energy transfer from $a^3\Sigma$; energy transfer to those states has an electronic energy defect of at least $\gtrsim$ 4 eV which must be converted into relative translational and vibrational energy in $SnO(X^1\Sigma)$. Such conversions apparently have a low probaility of occurring. Additionally, an extended spectrum, 250 nm $\leq \lambda \leq$ 800 nm, obtained at the highest [Sn] used, shows no evidence of Sn atomic emission. Thus the a priori unlikely two-step excitation of the Sn $^3P^o$ states which emit near 300 nm, is also not occurring rapidly.

In considering these quenching results in toto, the small quenching effect of N_2 on $SnO(A^3\Pi)$ appears somewhat anomalous. It seems unlikely that such an effect could occur for N_2, but not for N_2O. Although we do not presently understand the origin of this effect, it is so small that it seems unlikely to be important in the possible consideration of $SnO(A^3\Pi)$ as an upper chemical laser level.

The final quenching results obtained pertain to product quenching. These three preliminary observations are the measurements that suggest a possible hindrance in the use of the Sn/N_2O reaction as a chemical laser pump. Analysis of these results indicates that the quenching probably originates from a secondary reaction product and may not have a serious effect on the potential of an Sn/N_2O chemical laser. These observations need to be verified in detail; experimental verification appears feasible using HTFFR techniques and should be undertaken. In addition to such experimental studies, extended gain calculations

which include quenching by reaction products should be made. Such an effort was beyond the scope of the present effort, and was not warranted on the basis of these scanty preliminary data.

C. Kinetics and Mechanism of the Sn/N_2O Chemiluminescence

1. The Possible Participation of Reactant Excited States

In terms of its reaction kinetics, the strong temperature dependence and relatively small pre-exponential of $k_1(T)$ appear anomalous (refs. 6,8) for a simple, highly exothermic abstraction reaction. In order to tailor reaction conditions to make most efficient use of the reagents for laser application, it is desirable to attempt to understand the origin of this T-dependence. It seems probable that it arises, at least in part, from the increased participation of low-lying reactant excited states as the equilibrium concentrations of such species increase with the temperature. It is well known (e.g. refs. 24, 34-37) that the reactivities of electronically or vibrationally excited reagents can differ significantly from those of the ground state. For example, Menzinger and co-workers (ref. 35) have obtained evidence that the Ba/N_2O photon yield may be enhanced by vibrationally exciting the N_2O in the bending mode (ν_2 fundamental at 1.7 kcal). Menzinger suggests that the similar structure of N_2O in that mode to N_2O^- indicates the participation of a harpooning mechanism in the reaction. Atomic reagent electronic states, e.g., spin-orbit (J) states can have similar effects. For example, Braun et al (ref. 36) attribute a non-Arrhenius dependence of observed chemiluminescence intensity in the Pb/O_3 reaction to participation of super-equilibrium concentrations of $Pb(^3P_1)$. Zare and co-workers (ref. 9) reach a similar conclusion from their study of the same reaction. We have also found that removal rates of $Sn(^3P_1)$ by N_2O and O_2 (section III.B) are more rapid than the corresponding $Sn(^3P_0)$ reaction rates, in agreement with the results of Wiesenfeld et al (ref. 24) on $Sn(^3P_1)$ removal by a variety of reagents.† In addition, based on state correlation arguments, Wiesenfeld (refs. 22,38) has predicted that the Sn/N_2O reaction proceeds only through reaction of $Sn(^3P_{1,2})$ and that $Sn(^3P_0)$ (ground state) does not react with N_2O.

† Neither experiment distinguishes whether the removal by O_2 (or N_2O) is by physical quenching or reaction.

In the case of the Sn/N_2O reaction, there are markedly close matches between the value of the activation energy (6 ± 2 kcal) and the energies of low-lying N_2O vibrational states; e.g., the $3\nu_2$ and ν_3 (asymmetric stretch) modes of N_2O lie at 5.1 and 6.4 kcal, respectively--identical within experimental error with the observed activation energy. The $Sn(^3P_1)$ state lies at 4.9 kcal, which is again identical with observed activation energy within experimental error. To a first approximation (i.e., neglecting the temperature dependence of the partition function[†]), the equilibrium populations of these states and the rate coefficient will grow at the same rate with increasing temperature of the reaction zone. In view of these correlations and of the known differences in reactivity between excited and ground state reactants which occur in many systems, there appears to be a reasonable basis for speculating that the observed temperature dependence of the Sn/N_2O reaction rate coefficient arises, at least in part, due to the participation of excited reagents.

2. Low Pressure Dependence of Sn/N_2O Chemiluminescence

As indicated in section III.D.1, the observed increase of the $\Phi(a)$ and $\Phi(A)$ with bath gas pressure up to ≈ 15 torr may indicate that SnO(a,A) are formed from excited precursor molecules. However, the possible interference of collisional deactivation of the emitting states themselves at the HTFFR walls cannot be ruled out on the basis of the present data and would lead to a similar pressure-dependence. A real pressure dependence would affect the design and performance of a practical laser device based on the Sn/N_2O reaction; e.g., sufficient time (distance in a flowing system) would have to be allowed for this process to occur and higher pressures than might otherwise be needed would have to be used to rapidly convert the precursor to optically emitting states. However if the observed pressure dependence is an artifact of the flow tube experiment, these constraints will not apply and the laser design will be facilitated. It is necessary that further experiments, specifically to distinguish between these effects, be carried out before detailed mechanistic arguments can be advanced and before such arguments can be applied to practical laser design.

[†] These changes in the electronic and vibrational partition functions are within the range of experimental error in the present $k_1(T)$ data; more extensive, accurate measurements of $k_1(T)$ would reveal such effects.

3. Identification of SnO States

The evidence of section III. F suggests that the Sn/N_2O reaction produces only the SnO $a\,^3\Sigma^+$ (1) and $A\,^3\Pi$ (0^+) states, while the $B\,^3\Pi$ (1) and $D\,^1\Pi$ states are populated in a reaction between Sn and a product formed from N_2O at $T > 1000$ K, presumably O atoms. While the Sn/N_2O reaction has sufficient energy to populate the B and D states it is apparently state selective--a property in part responsible for the high $\Phi(a)$ and $\Phi(A)$ observed and hence in part responsible for the promise this reaction offers for an electronic transition laser. An explanation for this state selectivity is that the formation of triplet states is spin-allowed in the Sn/N_2O reaction while that of singlet states is spin-forbidden, though the spin rules are not rigid for a reaction involving a relatively heavy element such as Sn. The fact that the B and A states are not formed in the same reactions make it unlikely that they are two angular momentum components of the same triplet state; we must therefore question the state assignment of Zare et al (ref. 9). A similar conclusion was drawn by Linevsky and Carabetta (ref. 15) on the basis of the appearance of the A and B states in different flame zones of $SnCl_4/H_2/N_2O$ self-sustaining flames. If the B state is a singlet state, it could explain its occurrence in the same reaction as the D state. By analogy to the SiO and GeO identifications (refs. 39,40) the $A\,^3\Pi$ (0^+) state could in view of this evidence better be named $b\,^3\Pi$.

APPENDIX

OPTICAL GAIN

The emission from the Sn/N_2O reaction is dominated by $a^3\Sigma \rightarrow X^1\Sigma$ radiation for which the photon yield ≈ 0.5. The method for calculating zero-power optical gain between these electronic levels is given in this appendix for systems in which Sn and N_2O are rapidly reacted and in which gain can be observed before relaxation through electronic quenching or radiation can occur.

For Doppler-broadened lines, zero-power optical gain for transitions between the $a^3\Sigma$ and $X^1\Sigma$ levels is given by (refs. 32,33)

$$\gamma = \beta \frac{3}{4(2\pi)^{3/2}} \left(\frac{m}{kT}\right)^{1/2} \frac{S(J',J'')}{\tau \nu^3} \left[\frac{R_e^2(r)\, q(v',v'')}{\sum_{v''} R_e(r)\, q(v',v'')}\right] \left\{ \frac{1}{2J'+1} \left[SnO(a^3\Sigma)\right]_{v',J'} - \frac{3}{2J''+1} \left[SnO(X^1\Sigma)\right]_{v'',J''} \right\} \tag{A-1}$$

where β is the fractional isotopic abundance of the particular Sn isotope considered (β for $^{120}SnO = 0.33$), m is the mass of the molecule, $S(J',J'')$ the Honl-London factor for the transition, ν the wavenumber of the transition and $\tau^{-1}\left[\frac{R_e^2(r)\, q(v',v'')}{\sum_{v''} R_e^2(r)\, q(v',v'')}\right]$ is the transition probability for the transitions $SnO(a^3\Sigma)_{v'} \rightarrow SnO(X^1\Sigma)_{v''}$.

Spectroscopic constants for the states of interest are (refs. 2,15) (using the notation of Herzberg, reference 41):

$SnO(a^3\Sigma)$	$SnO(X^1\Sigma)$
$B' = 0.28\ cm^{-1}$	$B'' = 0.36\ cm^{-1}$
$G_o'(v') \approx \omega_o'v' \approx 499\ v'\ cm^{-1}$	$G_o''(v'') \approx \omega_o''v'' \approx 819\ v''\ cm^{-1}$
$\nu_{oo} = 20622\ cm^{-1}$	

It is assumed that, at the (bath gas) temperature, the vibrational-rotational distributions for both states are Boltzmann. This is not unreasonable since experimentally it is observed that the emission is primarily from the v = 0 levels of a $a^3\Sigma$ for 500 K < T < 1000 K indicating that (i) vibrational relaxation to the bath temperature is rapid compared to the radiative process and/or (ii) the $a^3\Sigma$ is formed with little vibrational excitation. Then the fractional population of SnO in a particular vibration-rotation state compared to the total population in a given electronic state, T, is given by

$$\frac{[SnO(T, v,J)]}{\sum_{v,J} [SnO(T, v,J)]} \approx \frac{hc\,B}{kT} \left[(2J + 1) \exp[- BJ(J + 1)hc/kT]\right] \times \frac{\exp[- G_o(v)\ hc/kT]}{1 + \exp[-G_o(1)\ hc/kT]} \qquad (A\text{-}2)$$

where the classical limit for the rotational partition function is used and only the first two terms of the vibrational partition function are retained.

REFERENCES

1. Felder, W. and Fontijn, A., "High-Temperature Fast-Flow Reactor Study of Sn/N_2O Chemiluminescence," Chem. Phys. Lett., 34, p. 398, 1975.

2. Suchard, S.N., Spectroscopic Data, Vol. 1, Part B, Plenum Press, New York, 1975.

3. Meyer, B., Smith, J.J. and Spitzer, K., "Phosphorescent Decay Time of Matrix-Isolated GeO, GeS, SnO and SnS and the Lifetimes of the Cameron Bands of CO-Type Diatomics," J. Chem. Phys., 53, p. 3616, 1970.

4. Fontijn, A., Kurzius, S.C., Houghton, J.J. and Emerson, J.A., "Tubular Fast-Flow Reactor for High Temperature Gas Kinetic Studies," Rev. Sci. Instr., 43, p. 726, 1972.

5. Fontijn, A., Kurzius, S.C. and Houghton, J.J., "High-Temperature Fast-Flow Reactor Studies of Metal-Atom Oxidation Kinetics," Fourteenth Symposium (International) on Combustion, The Combustion Institute, Pittsburgh, p. 167, 1973.

6. Fontijn, A., Felder, W. and Houghton, J.J., "Homogeneous and Heterogeneous Kinetics of the Al/O_2 Reaction in the 1000-1700 K Range," Fifteenth Symposium (International) on Combustion, The Combustion Institute, Pittsburgh, p. 775, 1975.

7. Felder, W. and Fontijn, A., "High-Temperature Fast-Flow Reactor Kinetic Studies. The AlO/O_2 Reaction near 1400 K," J. Chem. Phys., 64, p. 1977, 1976.

8. Fontijn, A., Felder, W. and Houghton, J.J., "HTFFR Kinetics Studies. The Temperature Dependence of Al/O_2 and AlO/O_2 Kinetics from 300 to 1700/1400 K," Sixteenth Symposium (International) on Combustion, The Combustion Institute, Pittsburgh, in press.

9. Oldenborg, R.C., Dickson, C.R. and Zare, R.N., "A New Electronic Band System of PbO," J. Molec. Spectr., 58, p. 283, 1975.

10. Fontijn, A., "Elementary Combustion Reaction Kinetic Measurements over Large Temperature Ranges, The HTFFR Technique," AIAA Paper 76-131, January 1976.

11. Moore, C.E., Atomic Energy Levels, NBS Circular 467, Vol. III, p. 75, 1958.

12. Edelstein, S.A., Eckstrom, D.J., Perry, B.E. and Benson, S.W., "Chemiluminescence Studies. III. Pressure Dependent Photon Yields for Several Metal-N_2O Reactions," J. Chem. Phys., 61, p. 4932, 1974.

13. Palmer, H.B., Krugh, W.D. and Hsu, C.J., "Chemiluminescent Spectra and Light Yields from Several Low-Pressure Diffusion Flames of Alkaline-Earth Metal Vapors," Fifteenth Symposium (International) on Combustion, The Combustion Institute, Pittsburgh, p. 951, 1975.

14. Fontijn, A., Meyer, C.B. and Schiff, H.I., "Absolute Quantum Yield Measurememts of the NO-O Reaction and Its Use as a Standard for Chemiluminescence Reactions," J. Chem. Phys., 40, p. 64, 1964.

15. Linevsky, M.J. and Carabetta, R.A., Chemical Laser Systems, Final Technical Report No. 75SDS4271, General Electric Space Sciences Laboratory, Valley Forge, PA, October 1975.

16. De Zafra, R.L. and Marshall, A., "Lifetimes and Oscillator Strengths for the $^3P_1{}^o$ Atomic States of Pb and Sn," Phys. Rev., 170, p. 28, 1968.

17. Wagenaar, H.C., Novotny, I. and deGalan, L., "The Influence of Hollow-Cathode Lamp Line Profiles upon Analytical Curves in Atomic Absorption," Spectrochim. Acta, 29B, p. 301, 1974.

18. Mitchell, A.C.G. and Zemansky, M.W., Resonance Radiation and Excited Atoms, Cambridge University Press, Cambridge, 1961.

19. Lin, C.L., Parkes, D.A. and Kaufman, F., "Oscillator Strengths of the Resonance Transitions of Ground-State N and O," J. Chem. Phys., 53, p. 3896, 1970.

20. Fontijn, A., Golomb, D. and Hodgeson, J.A., "A Review of Experimental Measurement Methods Based on Chemiluminescence," Chemiluminescence and Bioluminescence, M.J. Cormier, D.M. Hercules and J. Lee, Eds., Plenum Press, New York, p. 393, 1973.

21. Felder, W., Gould, R.K. and Fontijn, A., Kinetic Measurements on the Fate of Electronically Excited BaO from the Ba/N_2O Chemical Laser Candidate Pumping Reaction, Final Report, AeroChem TP-325, AFWL TR-75-218, AeroChem Research Laboratories, Princeton, NJ, July 1975.

22. Wiesenfeld, J.R., Cornell Univ., private communication to A. Fontijn, June 1976.

23. Baulch, D.L., Drysdale, D.D. and Horne, D.G., Evaluated Kinetic Data for High Temperature Reactions, Vol. 2, CRC Press, Cleveland, p. 69, 1973.

24. Foo, P.D., Wiesenfeld, J.R., Yuen, M.J. and Husain, D., "Collisional Quenching of Electronically Excited Tin Atoms, Sn($5p^2$ $^3P_1$) and Sn($5p^2$ $^3P_2$), by Time-Resolved Attenuation of Atomic Resonance Radiation," J. Phys. Chem., 80, p. 91, 1976.

25. Field, R.W., Jones, C.R. and Broida, H.P., "Gas Phase Reaction of Ba with N_2O. II. Mechanism of the Reaction," J. Chem. Phys., 60, p. 4377, 1974.

26. Hsu, C.J., Krugh, W.D. and Palmer, H.B., "Pressure Dependence of the $A(^1\Sigma) \rightarrow X(^1\Sigma)$ Photon Yield in the Reactions of Ba(g) with N_2O and NO_2," J. Chem. Phys., 60, p. 5118, 1974.

27. Fontijn, A. and Johnson, S.E., "Mechanism of CO Fourth Positive VUV Chemiluminescence in the Atomic Oxygen Reaction with Acetylene. Production of $C(^3P, ^1D)$," J. Chem. Phys., 59, p. 6193, 1973.